

Predicting the axial compressive capacity of circular concrete filled steel tube columns using an artificial neural network

Mai-Suong T. Nguyen^{1,2a}, Duc-Kien Thai^{1b} and Seung-Eock Kim^{*1}

¹Department of Civil and Environmental Engineering, Sejong University, 98 Gunja-dong, Gwangjin-gu, Seoul 05006, South Korea

²Thuyloi University, 175 Tay Son, Hanoi, Vietnam

(Received December 24, 2019, Revised April 7, 2020, Accepted April 10, 2020)

Abstract. Circular concrete filled steel tube (CFST) columns have an advantage over all other sections when they are used in compression members. This paper proposes a new approach for deriving a new empirical equation to predict the axial compressive capacity of circular CFST columns using the Artificial Neural Network (ANN). The developed ANN model uses 5 input parameters that include the diameter of circular steel tube, the length of the column, the thickness of steel tube, the steel yield strength and the compressive strength of concrete. The only output parameter is the axial compressive capacity. Training and testing the developed ANN model was carried out using 219 available sets of data collected from the experimental results in the literature. An empirical equation is then proposed as an important result of this study, which is practically used to predict the axial compressive capacity of a circular CFST column. To evaluate the performance of the developed ANN model and the proposed equation, the predicted results are compared with those of the empirical equations stated in the current design codes and other models. It is shown that the proposed equation can predict the axial compressive capacity of circular CFST columns more accurately than other methods. This is confirmed by the high accuracy of a large number of existing test results. Finally, the parametric study result is analyzed for the proposed ANN equation to consider the effect of the input parameters on axial compressive strength.

Keywords: axial compressive capacity; concrete filled steel tube; empirical equation; artificial neural network; parametric study

1. Introduction

In recent decades, concrete filled steel tube (CFST) columns have been increasingly used in construction, such as with civil structures, buildings, and bridges (Shanmugam and Lakshmi 2001, Tao *et al.* 2007, Uy 2001, Varma *et al.* 2002). A CFST column is the composite structure of a steel tube that is filled in with concrete. Many researchers have found that a CFST column has advantages over the conventional steel or reinforced concrete column due to its high-strength, stiffness, ductility, fire resistance and better seismic resistance (Aslani *et al.* 2015, Aslani *et al.* 2016a, Aslani *et al.* 2016b, Tang 2017, Wang *et al.* 2018, Ekmekyapar and Hasan 2019). Therefore, the use of a CFST column in different areas of construction is becoming a prevalent solution.

To estimate the ultimate strength of CFST columns, different design codes have been developed such as (ACI 318 1962), (EC4 2004), and (AIJ 1997). These criteria all provide practical design equations, which however do not agree well with experimental data due to their high safety

factors and their limited applicable range of configuration parameters. For several years, a host of theoretical and experimental studies on CFST columns under an axial load is developed (Abed *et al.* 2013, Schneider 1998, Xiao 1989). Schneider (1998) executed an experimental and analytical study on the behaviour of a short column that had different shapes and depth-tube wall thickness ratios subjected to a compression load. Xiao (1989) conducted a series of CFST column tests and then proposed a tri-axial constitutive relationship. (Abed *et al.* 2013) tested CFST columns under pure axial loading with different diameter-to-thickness ratios and concrete's compressive strength. These studies determine the axial compressive strength of CFST columns based on a narrow range of material properties and geometry configurations while the relationship between the CFST compressive strength and configuration parameters is nonlinear and complex. Moreover, none of them provided an explicit equation for practical design. Therefore, a new method is still needed, which can overcome all the above limitations.

In recent years, literary publications in the field of civil engineering have shown that various engineering problems can be addressed using artificial intelligence technique (AI) (Cheng and Cao 2014, Yaseen *et al.* 2018, Luat *et al.* 2020a), particularly artificial neural network (ANN) (Dantas *et al.* 2013, Duan *et al.* 2013, Das and Choudhury 2019, Hasan *et al.* 2019, Luat *et al.* 2020b). ANN is one of the most popular soft computing techniques, and thanks to its adaptive nature, is able to learn, generalize, categorize

*Corresponding author, Professor
E-mail: sekim@sejong.ac.kr

^a Ph.D. Student
E-mail: suonngtm@sju.ac.kr

^b Ph.D.

and predict targets. Duan *et al.* (2013) successfully used an artificial neural network (ANN) to predict the compressive strength of recycled aggregate concrete. Dantas *et al.* (2013) applied an ANN to determine the compressive strength of concrete containing construction and demolition waste with an acceptable error range. Lee and Lee (2014) presented a theoretical model based on an ANN for the estimated shear strength of slender fiber reinforced polymer (FRP) reinforced concrete flexural members without stirrups. The ANN model has therefore been demonstrated as an effective method that provides a feasible solution in axial compressive capacity prediction of circular CFST column.

In this study, an ANN model is developed to predict the axial compressive capacity of CFST columns. Five input parameters are used to describe attributes defined by diameter of the column (D), length of the column (L), thickness of the steel tube (t), the concrete compressive strength (f'_c), and steel yield strength (f_y) and one output variable is the axial compressive strength (N_u). A total of 219 available data are collected for training and testing process. The predictive performance of ANN is then compared by three well-known design codes and the other AI models. Performance assessment results are quantified by evaluation criteria. The obtained results show the feasibility and superiority of the developed ANN model. It is also noteworthy that proposed ANN model successfully solved the limitations of the design codes and existing experimental researches. An explicit formulation is derived from ANN's parameters for design purposes. Finally, the parametric study investigates the effects of input configuration parameters on CFST strength.

The rest of the paper is organized as follows. In Section 2, the available design codes to determine CFST column strength is briefly described. A general introduction of the dataset and its statistics are presented in Section 3. The architecture and parameters of the ANN model are analyzed and highlighted in Section 4. Section 5 assesses the performance of the proposed ANN model, and Section 6 proposes a potential empirical equation, discusses performance comparisons and analyzes the effects of certain parameters on experimental-to-predicted strength ratio. The parametric study is described in Section 7, and the most important parameter is clarified in Section 8. Finally, the conclusions are provided in Section 9.

2. Empirical equation for CFST columns in design codes

An overview of the available scientific literature of the related standards about the CFST columns is given below. These discussed formulations are used for the comparison with the proposed model. For the sake of consistency, the same notations are used for the similar terms in each design code and are summarized in the Nomenclature. The values calculated from each code are denoted by the superscript, such as N_{EC4} , N_{ACI} , and N_{AII} .

2.1 Eurocode 4 (EC4)

The EC4 design standard (EC4 2004) provides an equation to determine the ultimate compressive capacity of a CFST column, which is based on limit state concepts. Eurocode 4 determines the resistance capacity by considering the contribution of the steel tube section, the section of concrete and the confinement of concrete by the steel tube. The concrete strength is increased by a factor of η_c due to the occurrence of a tri-axial state of the stress condition while the steel tube strength is reduced by the coefficient η_a since the hoop stresses cause a reduction in the effective yield stress of the steel. Thus, the axial capacity in the compression of the column is determined by the following equation

$$N_{EC4} = \left(1 + \eta_c \frac{t}{D} \frac{f_y}{f'_c} \right) f'_c A_c + \eta_a f_y A_s \quad (1)$$

where

$$\eta_c = 4.9 - 18.5\lambda + 17\lambda^2, \eta_c \geq 0 \quad (2)$$

$$\eta_a = 0.25(3 + 2\lambda), \eta_a \leq 1 \quad (3)$$

$$\lambda = \sqrt{\frac{N_{pl,R}}{N_{cr}}}; N_{pl,R} = f_y A_s + f'_c A_c \quad (4)$$

$$N_{cr} = \frac{\pi^2 (EI)_{eff}}{l^2}; (EI)_{eff} = E_s I_s + K_e E_c I_c \quad (5)$$

where η_c is the coefficient of the concrete confinement, η_a is the coefficient of the steel tube confinement, t is the thickness of the steel tube, D is the diameter of the column, f'_c is the concrete compressive strength, f_y is the steel yield strength, A_c is the cross-section area of the concrete, A_s is the cross-section area of the steel, λ is the relative slenderness, and l and $(EI)_{eff}$ are the buckling length of the column and the effective flexural stiffness, respectively. K_e is the correction factor, $K_e = 0.6$.

Modulus of elasticity of concrete

$$E_{c2} = 22000 \left[(f'_c + 8) / 10 \right]^{0.3} \text{ MPa} \quad (6)$$

For relative slenderness equal to zero $\lambda=0$, the axial load of the section is simplified to

$$N_{EC4} = \left(1 + 4.9 \frac{t}{D} \frac{f_y}{f'_c} \right) f'_c A_c + 0.75 f_y A_s \quad (7)$$

2.2 American Concrete Institute (ACI)

The ACI (ACI 1962) is the formula to calculate the axial compressive capacity of a CFST column. The formulation does not cover the effect of the thickness of the steel tube, concrete confinement and the interaction between the concrete core and steel tube.

The ultimate axial load is determined by

$$N_{ACI} = 0.85 A_c f'_c + A_s f_y \quad (8)$$

where f_c' is the strength of the concrete, f_y is the yield strength of the steel, A_c is the cross-section area of the concrete, and A_s is the cross-section area of the steel.

2.3 Architectural Institute of Japan (AIJ)

According to the Architectural Institute of Japan AIJ (AIJ 1997), the ultimate compressive strength of a steel tube filled with concrete under an axial load is determined by the following equation:

$$N_{AIJ} = 0.85f_c'A_c + (1 + \eta)f_yA_s \quad (9)$$

where f_c' is the concrete compressive, f_y is the steel yield strength, A_c is the cross-section area of the concrete, and A_s is the cross-section area of the steel. In this equation, the confinement factor ($\eta = 0.27$) is acknowledged to illustrate the interaction between the steel tube and the concrete filling, which provides the enhancement of the load-carrying capacity.

2.4 Limitation of design codes

The design codes have provided some limitations on the material properties and the slenderness conditions, which are summarized in Table 1. The use of high strength materials is still limited in EC4, which is only applicable to a steel yield stress up to 460 MPa and a concrete cylinder compressive strength up to 50 MPa. High strength materials are now recommended in the AIJ with the upper limits for the strengths of concrete being extended to 60 MPa. A larger range for the material strengths is specified in the ACI with a minimum concrete compressive strength of 17.2 MPa. Another contributing factor to the limitations of the design codes is the diameter to thickness (D/t) ratio. Namely, the maximum D/t of ACI and AIJ are limited by

$$\sqrt{8E_s / f_y} \text{ and } 150 \sqrt{\frac{235}{f_y}}, \text{ respectively. EC4 considers the}$$

local buckling effect for circular thin-walled tubes by limiting the diameter (D) to thickness (t) ratio to $90 \sqrt{\frac{235}{f_y}}$,

where f_y is the steel yield strength. However, no details were given in the EC4 on how to account for the local buckling effect if these limits were exceeded.

Table 1 The prediction methods and related limitations

Design code	D/t	f_y (MPa)	f_c' (MPa)
EC4	$D/t \leq 90 \sqrt{\frac{235}{f_y}}$	$235 \leq f_y \leq 460$	$20 \leq f_c' \leq 50$
ACI	$D/t \leq \sqrt{8E_s / f_y}$	$f_y \leq 345$	$f_c' \geq 17.2$
AIJ	$D/t \leq 150 \sqrt{\frac{235}{f_y}}$	$235 \leq f_y \leq 355$	$f_c' \leq 60$

Table 2 Range of parameters in the experimental dataset

Input	Range			
	Minimum	Maximum	Mean	Standard deviation
D (mm)	25.40	450.10	162.36	94.21
L (mm)	216.00	4000.00	922.01	690.08
t (mm)	0.70	12.80	4.41	2.63
f_y (MPa)	168.21	853.00	388.60	139.23
f_c' (MPa)	18.04	52.20	31.61	9.20
Output				
N_u (kN)	14.40	9835.00	2102.88	2305.25

3. Description of the selected dataset

In this study, a total of 219 experimental data is collected from the available technical literature: (Salani and Sims 1964, Furlong 1967, Knowles 1970, Tomii 1977, Lin 1988, Xiao 1989, Hayashi 1990, Luksha 1991, Schneider 1998, Yamamoto *et al.* 2000, O'Shea and Bridge 2000, Sakino *et al.* 2004, Giakoumelis and Lam 2004, Zeghiche and Chaoui 2005, Gupta *et al.* 2007, Yu *et al.* 2008, WLA Oliveira 2008, Beck *et al.* 2009, Li *et al.* 2016) and is presented in Appendix A. The developed ANN model have five input parameters that consist of the diameter of column (D), the column length (L), the thickness of the steel tube (t), the yield strength of steel (f_y), and the compressive strength of concrete (f_c'). The axial compressive capacity (N_u) serves as an output variable. A summary of input and output values is presented in Table 2.

The distribution of each considered parameters is demonstrated in Fig. 1. It can be seen that a large number of tests are used belongs to CFST columns with normal strength steel ($f_y \leq 460$ MPa with 79.5%) and normal strength concrete ($f_c' \leq 50$ MPa with 97.3%). Only a small number of tests have been carried out on high strength steel ($f_y > 460$ MPa with 20.5%) and high strength concrete (50 MPa $\leq f_c' \leq 90$ MPa with 2.7%). Namely, the concrete compressive strength ranges from 18.04MPa to 52.20 MPa and the steel yield strength varies from 168.21 MPa to 853 MPa. It is also observed that both the short columns and the slender columns are considered in this database. The short columns are defined as those with $L/D \leq 4$, where L is the length of the specimens and D denotes the outside diameter of a circular section, respectively. The remaining cases with $L/D > 4$ are considered as slender members. This classification is based on the recommendation given by (Goode 2008). The longest CFST column is reported by (Zeghiche and Chaoui 2005) with a length of 4000 mm, and the largest diameter of 450.10 mm is reported by (Yoshioka *et al.* 1995). The application thickness varied from 0.7 to 12.8 mm. It is observed that the input and output parameters can cover a wide range of reality construction.

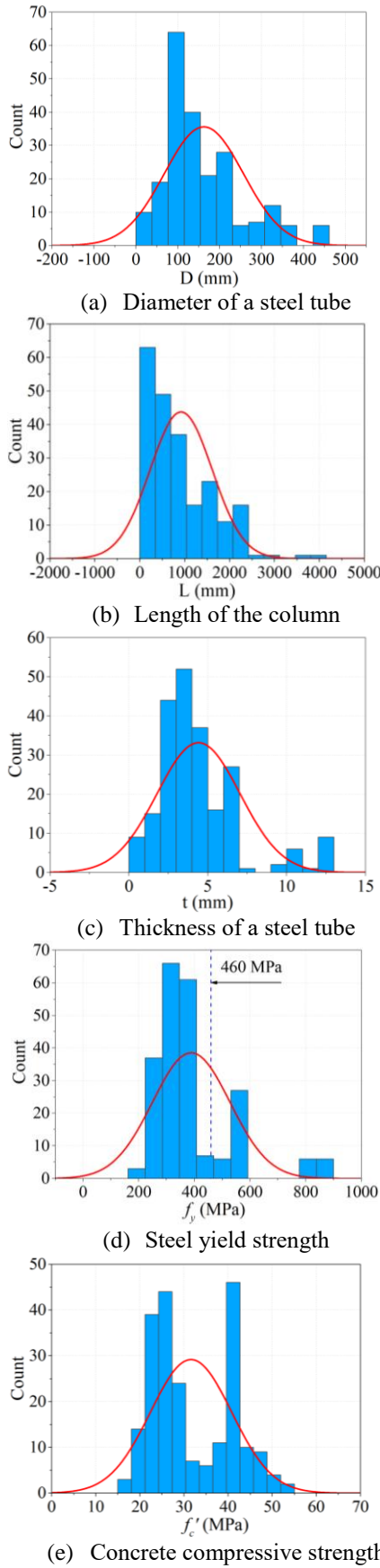


Fig. 1 Distribution of the experiment data

4. Development of the ANN model

4.1 Overview of the artificial neural network

An artificial neural network is a computational model that mimics the behavior of biological neurons that exist in the human brain. It has the capability to handle complex nonlinear relationships between input and output datasets. An ANN has several advantages, but one of the most recognized advantages is the fact that it can actually learn from observing data sets. An ANN takes data samples rather than entire data sets and sets them to training, which saves both time and money. ANNs are considered fairly simple mathematical models to enhance existing data analysis technologies.

One of the most popular neural networks is the layered feedforward neural network with a backpropagation algorithm. A typical structure of the ANN model consists of an input layer, one or more hidden layers, and an output layer, and each layer consists of numerous neurons, which is illustrated in Fig. 2.

Fig. 3. shows how information is processed through a single artificial neuron. Suppose there are n inputs (x_i with $i = 1, 2, 3, \dots, n$).

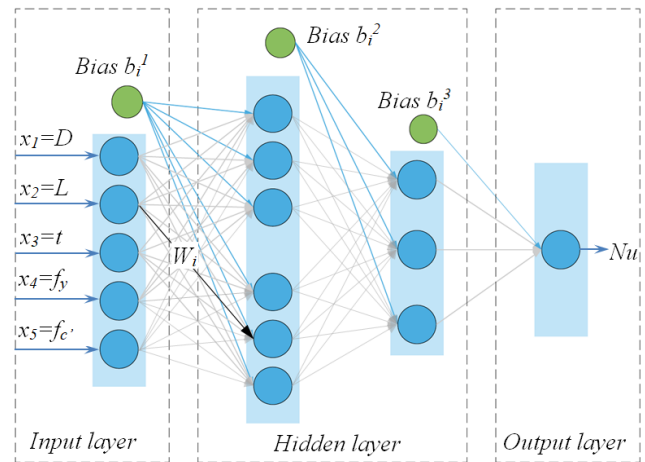


Fig. 2 Construction of the ANN model

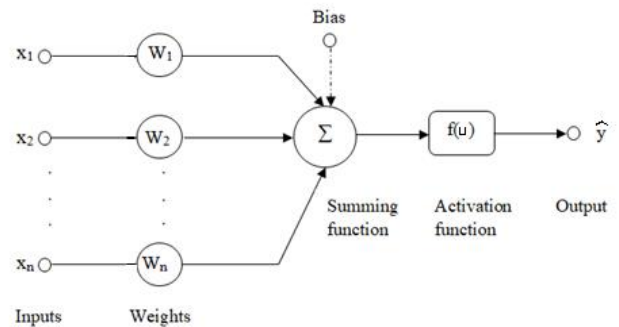


Fig. 3 Diagram of an artificial neuron

The weights connecting n numbers of inputs to j^{th} neuron are represented by w (w_i with $i = 1, 2, 3, \dots, n$). Each of the neurons determines a weighted sum of its input, passes the sum through its activation function, and presents the activation value to the output layer. Mathematically, the

sum can be described as $\sum_{i=1}^n x_i w_i$. The output of summing

may sometimes become equal to zero and to prevent this type of situation from occurring, a bias b is added to it. Following the computation of the sum with value as

$u = \sum_{i=1}^n x_i w_i + b$ is passed through its activation function f

and can produce an output value $y_i = f(u)$. Thus, regarding the above information the output and the value of output \hat{y}_i can be described as follows

$$\hat{y}_i = f(u) = f\left(\sum_{i=1}^n x_i w_i + b\right) \quad (10)$$

The activation function is a non-linear function between the inputs and the response variable (Ketkar 2017). There are three activation functions commonly used to develop an ANN model, which include Sigmoid, Hyperbolic Tangent (Tanh), and Rectified Linear Unit (ReLU) transfer functions. They are expressed by Eqs. (11)-(13), respectively, and illustrated in Fig. 4.

- Sigmoid transfer function (see Fig. 4(a))

$$f(x) = \frac{1}{1 + e^{-x}}, 0 \leq f(x) \leq 1 \quad (11)$$

- Hyperbolic tangent transfer function (see Fig. 4(b))

$$f(x) = \frac{e^x - e^{-x}}{e^x + e^{-x}}, -1 \leq f(x) \leq +1 \quad (12)$$

- Rectified linear unit function (see Fig. 4(c))

$$f(x) = \max(0, x) = \begin{cases} 0 & \text{for } x \leq 0 \\ x & \text{for } x > 0 \end{cases}, 0 \leq f(x) \leq \infty \quad (13)$$

The usage of activation functions in this study will be discussed in Section 4.2.

To evaluate the performance of the ANN model, the following criteria were used, which include the mean squared error (MSE), the root mean squared error (RMSE), the mean absolute percentage error (MAPE), the mean absolute error (MAE), the linear correlation coefficient (R) and the variance accounted for (VAF) are expressed by Eqs. (14)-(19), respectively.

$$MSE = \frac{1}{n} \sum_{i=1}^n (y_i - \hat{y}_i)^2 \quad (14)$$

$$RMSE = \sqrt{\frac{1}{n} \sum_{i=1}^n (y_i - \hat{y}_i)^2} \quad (15)$$

$$MAPE = \frac{100}{n} \sum_{i=1}^n \left| \frac{y_i - \hat{y}_i}{y_i} \right| \quad (16)$$

$$MAE = \frac{\sum_{i=1}^n (|y_i - \hat{y}_i|)}{n} \quad (17)$$

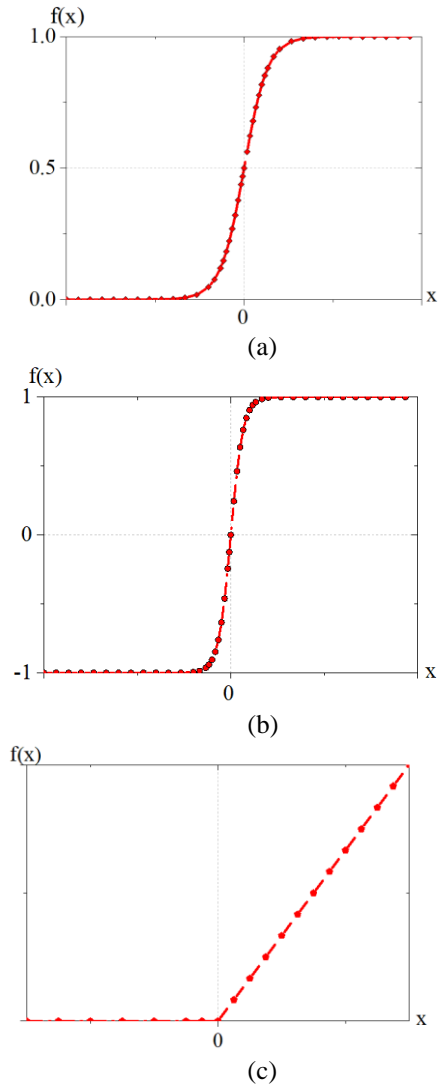


Fig. 4 Activation functions

$$R = \frac{n \sum_{i=1}^n (y_i \hat{y}_i) - \sum_{i=1}^n y_i \sum_{i=1}^n \hat{y}_i}{\sqrt{[n \sum_{i=1}^n y_i^2 - (\sum_{i=1}^n y_i)^2] [n \sum_{i=1}^n \hat{y}_i^2 - (\sum_{i=1}^n \hat{y}_i)^2]}} \quad (18)$$

$$VAF = \left(1 - \frac{var(y_i - \hat{y}_i)}{var(y_i)} \right) 100 \quad (19)$$

where y_i is the actual value, \hat{y}_i is the predicted value and n is the total number of samples, which is the dataset. The linear correlation coefficient (R) defines the fit of the predicted output to the experimental output. The linear correlation coefficient value of 1.0 means that the predicted values are exactly the same as the experimental values; whereas, for MSE, RMSE, MAPE, and MAE, the absolute accuracy between the predicted and the experimental values will yield the perfect value of 0.0. Another criterion, which is the VAF, should be close to 100%.

Table 3 Coefficients for normalization variables

Coefficients	Variables				
	D	L	t	f_y	f_c'
Average \bar{x}	162.922	895.533	4.539	393.137	31.464
Standard deviation σ	96.365	666.517	2.715	141.947	9.248

4.2 The proposed ANN model

4.2.1 Normalization of the data

In data processing, normalization is really necessary, because the neural networks require that their input and output data must be normalized to have the same order of magnitude. This step is generally performed during the data preprocessing step. In the normalizing process of the dataset, the values of the normalized variable are in the range between 0.0 and +1.0, and the average values are set to zero (Ioffe 2017). This technique is called the standardization, and it gives the normalization variable $x_{i,norm}$ by

$$x_{i,norm} = \frac{x - \bar{x}}{\sigma} \quad (20)$$

where $x_{i,norm}$ is the normalized variable, x is the original variable, \bar{x} is the average value of the variable, and σ is the standard deviation of the variable. The normalization coefficients for variables are presented in Table 3.

4.2.2 Construction of the ANN model

The network architecture and the parameter settings affect the performance of the ANN model, which may lead to the difficult task of optimizing the network architecture. Based on the trial and error method, the optimal parameters, which include the number of hidden layers, the neurons of a hidden layer, activation function, and learning rate are determined. With each epoch, the parameters are changed to obtain a respective error value. This process is repeated until the optimal parameters are reached with a minimum error.

Fig. 5 presents the procedure to optimize the developed ANN model using the Python programming language. As illustrated in Fig. 5, four different parameters are involved in the optimization of the training process. For each parameter, various values are considered, which include the number of hidden layers using 1, 2, 3 or 4, the number of hidden neurons ranging from 1 to 5, the values of the learning rate ranging from 0.01 to 0.15, and the activation function using *Sigmoid*, *Tanh* or *ReLU*. For the purpose of selecting the best parameter set, the mean squared error (MSE) is employed to estimate the performance of the ANN model. The results of optimizing the network process are presented in Fig. 6. It is noted that, when the value of a parameter for the neural network was changed, the values of other parameters didn't change.

The relationship between the MSE with respect to the number of hidden layers is analyzed in Fig. 6(a). In fact, the number of hidden layers is affected by the complexity of the problem. The more complex problem, the more numbers of hidden layers are required. However, it has been observed from the literature that one hidden layer is sufficient for most of the problems in civil engineering according to Altun *et al.* (2008), Hwang *et al.* (Hwang *et al.* 2019) and Kang *et al.* (2006). In the present study, the forward network with a hidden layer also proved suitable to solve the problem posed. This is clarified in Fig. 6(a), which is shown with both the training and the testing processes. When the number of hidden layers increases from 1 to 4, the value of the MSE significantly increases. The MSE increases 46.6% for the training and 68.2% for the testing. The lowest MSE is observed when the number of hidden layers is 1. It is concluded that one hidden layer is the best choice for the current ANN architecture.

Fig. 6(b) shows the result of the MSE corresponding to the number of neurons for the training set and the testing set. Even though there is no specific rule to determine the number of neurons (nodes) in a hidden layer, this number must be sufficient for the accurate modeling of the problem, and it should be sufficiently low to ensure generalization. The number of neurons can be found using the trial and error method. It is observed that the MSE decreased rapidly, which is at a rate of 56.9% for the training and 58.8% for the testing as the model utilized a range of hidden neurons from 1 to 3. When the model uses a range of hidden neurons varying from 3 to 5, the MSE alters insignificantly, 4.1% and 4.3 %, respectively. Thus, the neurons of the hidden layer could be equal to 3, 4, or 5. Besides, it needs to be repeated that one of our main goals is to derive a simple explicit formula of axial compressive strength for convenience in design calculations. For that reason, the three-neuron hidden layer is chosen as the most optimal model.

The activation function has a strong effect on predicting the performance of the model. In this study, three different activation functions are used for the training and the testing processes. Fig. 6(c) shows the performance of the model in terms of MSE as different activation functions. The ReLU function is a nonlinear function, which means we can easily back-propagate the errors and have multiple layers of neurons being activated by the ReLU function, so the ReLU function can be fast convergence. Fig. 6(c) also is shown that the usage of ReLU induces the lowest MSE. Therefore, the ReLU function is chosen for the proposed model.

In the back-propagation algorithm, the weights of the model are updated when the estimation of the error gradient for the current state of the model was finished.

The amount that the weights are updated during the training is referred to as the step size or the "learning rate". Specifically, the learning rate is a configurable hyper-parameter used in the training of neural networks that has a small positive value. Fig. 6(d) shows the effect of the learning rate on the performance of the current ANN model. It is found that while all the other learning rate values induce a similar value of the MSE, the value of 0.05 of the Adam optimization algorithm provides the lowest MSE.

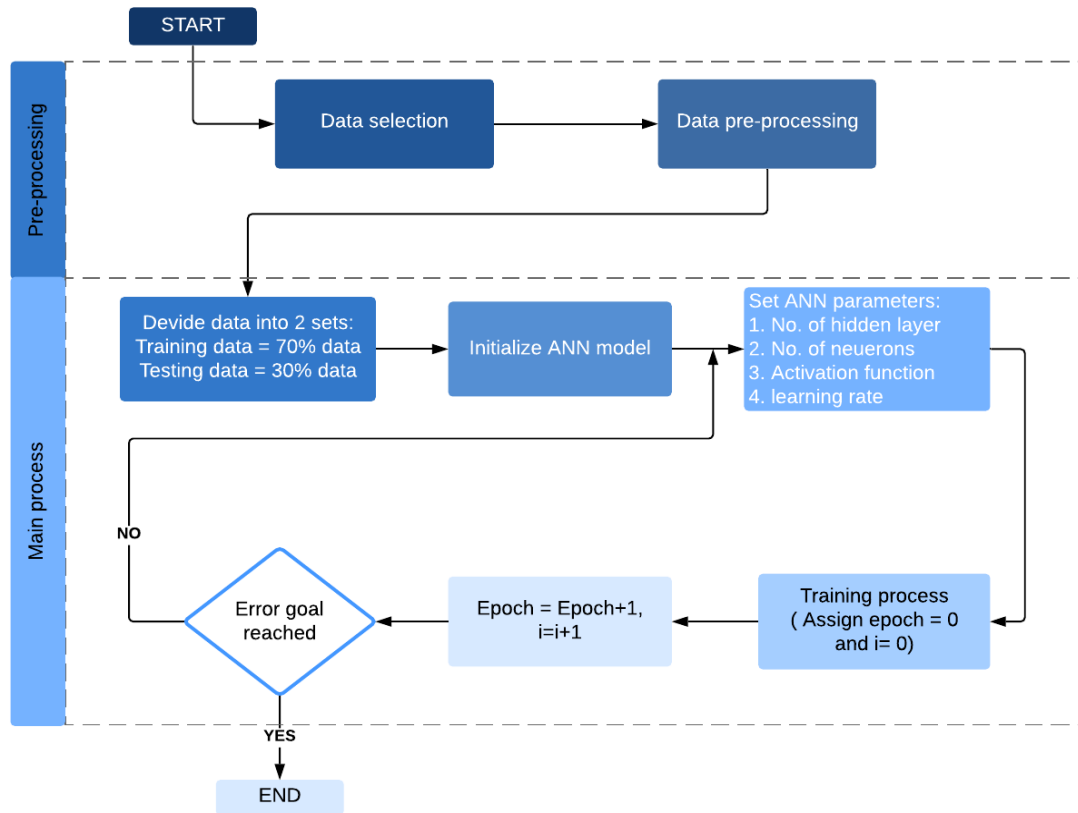


Fig. 5 Flowchart of the optimal model

Thus, the learning rate of 0.05 is used for further processes.

Fig. 6(e) indicates that the value of the epochs of 2000 is an optimized choice for all the cases because the epochs must be satisfactory to optimize the model, and they should be small enough to save time.

As discussed above, it can be seen that not only one hidden layer model, but also two, three, and four-hidden layer models with optimal parameters are carefully modeled. Finally, the ANN architecture of 5-3-1, which means that the optimal model has the one-hidden layer with five nodes in the input layer, three nodes in the hidden layer, and one node at the output of the network, is chosen for an optimal ANN model. Moreover, the selected network architecture and the parameters for the optimal ANN model are summarized in Table 4.

5. Performance of the proposed ANN model

This section presents the performance of the proposed ANN model, which includes the training and the testing performances. The linear correlation criteria presented in Section 4.1 is used to evaluate the accuracy of the ANN model.

Figs. 7(a)-7(c) show the performance of the proposed ANN model in regards to training, testing set, and all the data, respectively. It is observed that the data points closely matched a diagonal line, which represents the best correlation between the predicted and the measured values. For the training set, the correlation coefficient (R) of 0.992

is reached, which indicates that the correlations between the predictions and the actual data are very good. Even though the testing process is independent of the training process, the predicted results also show a robust correlation compared to the test data with a correlation coefficient of 0.992. This further proved that the ANN model could obtain accurate predictions for the values of data that were being investigated. Figs. 8(a) and 8(b) shows the comparison between the predicted and the measured for the training and the test set. It is found that the estimated N_u values are obtained from the ANN in the training set and the testing set closely matched the measured values. The excellent prediction performance shows the proposed models that can capture the complex nonlinear mapping between the five input variables and the ultimate axial capacity N_u .

Table 4 Selected parameters of the proposed model

Content	Value
Number of units in the input layer	5
Number of hidden layers	1
Number of units in hidden layer	3
Number of units in output layer	1
Epochs	2000
Activation function	ReLU
Optimization algorithm	Adam
Learning rate	0.05

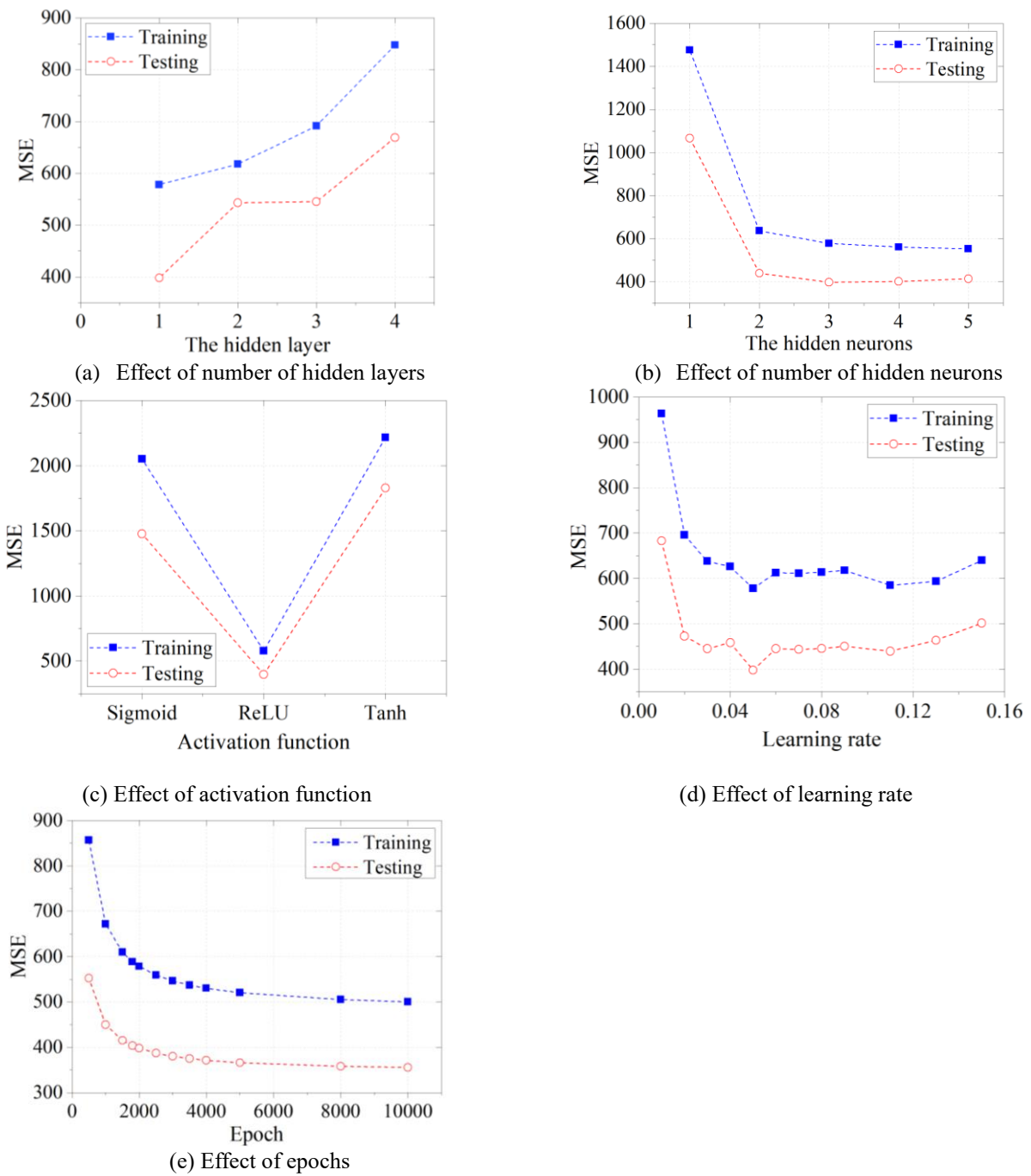


Fig. 6 Mean squared error* (MSE) as a function of the parameter (*Unit: $\times 10^2 \text{ kN}^2$)

The performance evaluation results of the ANN training set and the testing set are seen in Figs. 9(a) and 9(b). Obviously, R and VAF are close to 1, and MSE, RMSE, MAPE, and MAE are close to 0 in both datasets, which indicates that the prediction accuracy of the ANN is relatively high. These remarkable results can be considered as evidence for the reliability of the proposed model.

6. Empirical equation development

6.1 Developing the empirical equation

The main goal of this sub-section is to derive an explicit formulation to predict the axial compressive capacity of the CFST column. First, it is noted that, before the training process, all the input parameters were normalized using Eq. (20), which means that they are re-scaled. The normalized values are shown in Table 3.

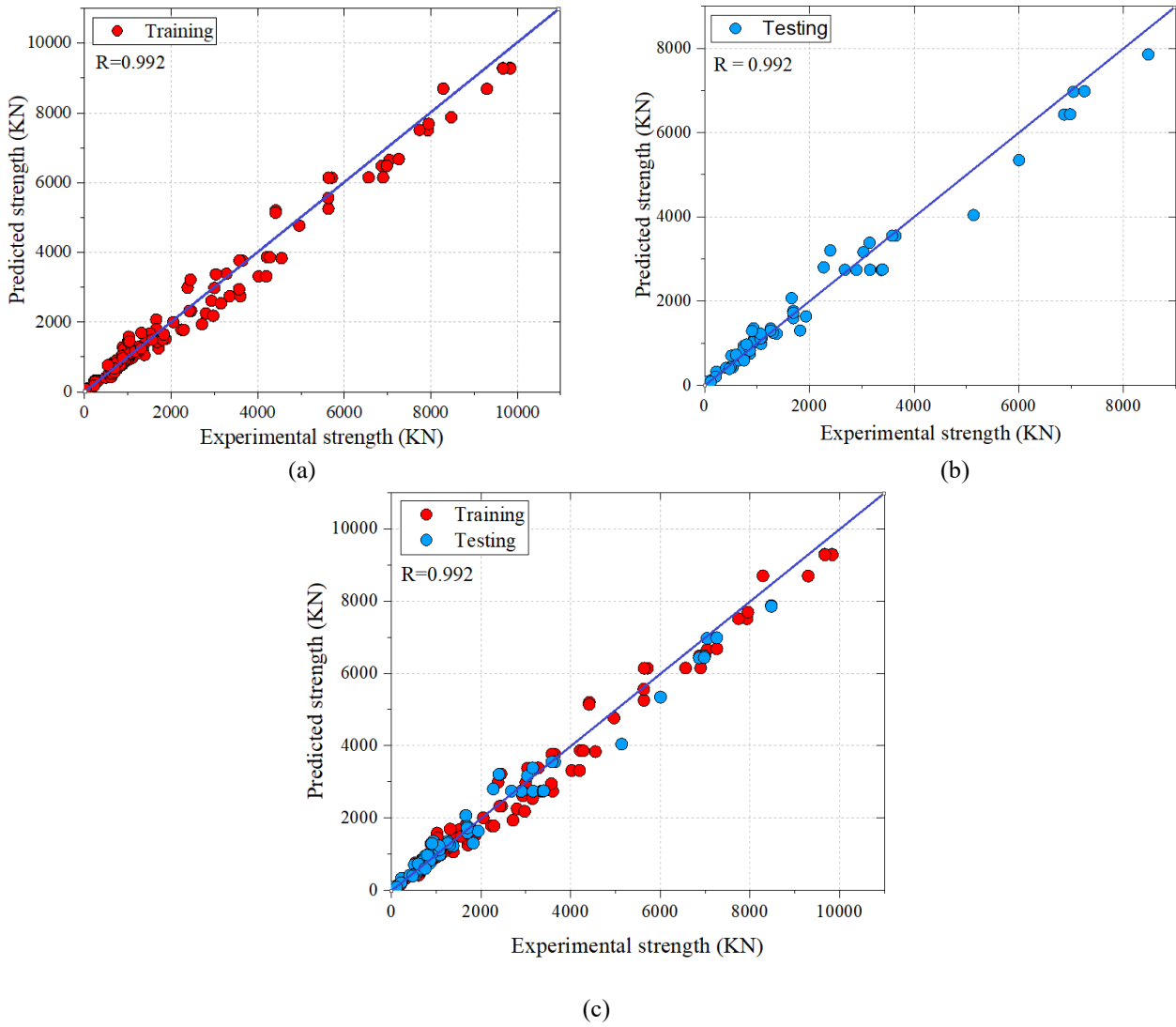
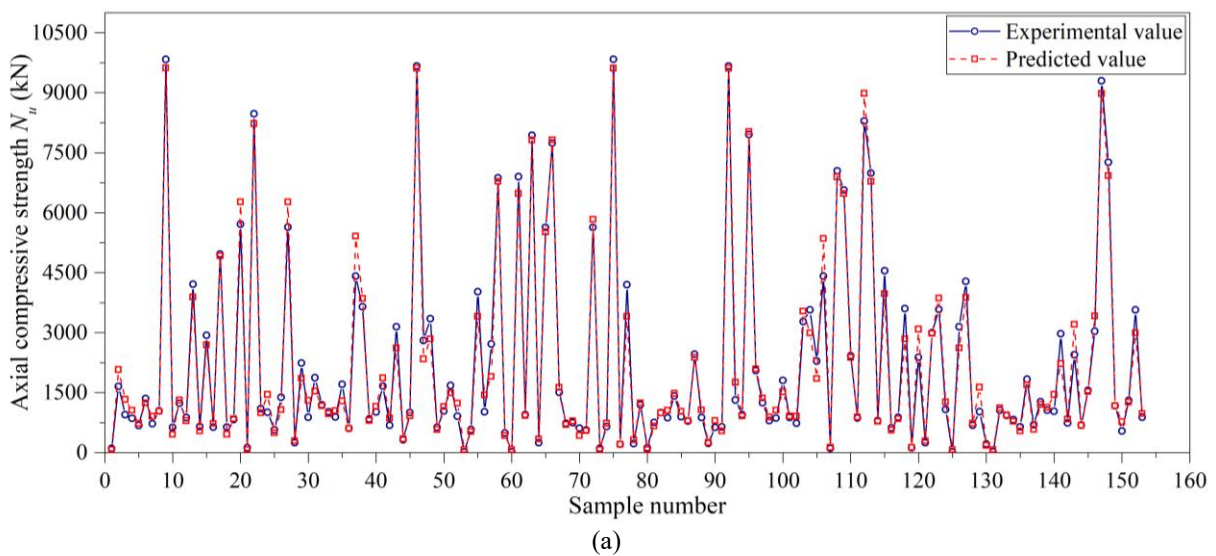
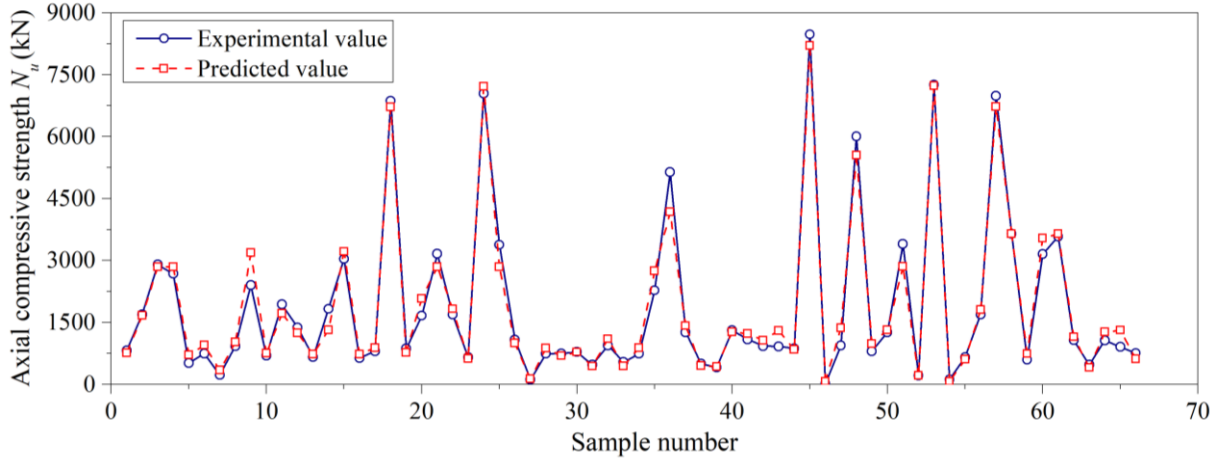


Fig. 7 Comparison between the actual and the predicted value for (a) training set, (b) the testing set and (c) all data



Continued-



(b)

Fig. 8 Experimental and predicted N_u values obtained from the ANN in (a) the training set and (b) the testing set

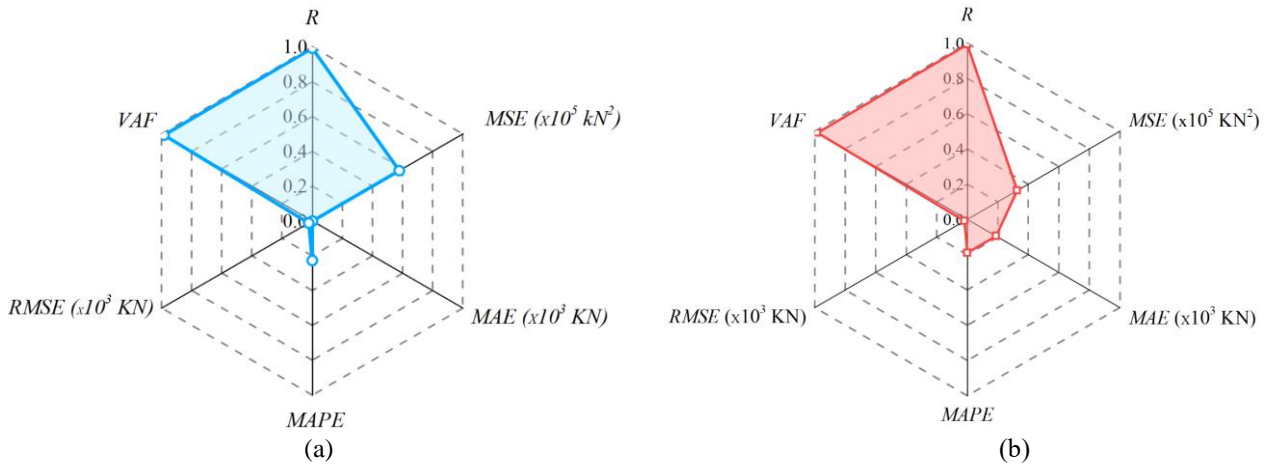


Fig. 9 Radar chart of the performance evaluation of the ANN in (a) the training set and (b) the testing set

Second, after the process of optimized ANN model finishes, the connection weights and the biases of the optimal ANN are obtained from PyCharm, which are presented in Table 5. Third, the axial compressive capacity is computed as a function of the input variables, including the diameter of the column (D), the length of column (L), the thickness of the steel tube (t), the compressive strength of the concrete (f'_c), and the yield strength of the steel (f_y).

Based on Eq. (10) in sub-section 4.1, and the values of the weights and the biases are shown in Table 5, the explicit formulation of axial compressive capacity of the CFST column is expressed as

$$N_u = 10.731 * \max(0, Z_1) + 5.122 * \max(0, Z_2) + 8.232 * \max(0, Z_3) + 7.091 \quad (21)$$

The values of 10.731, 5.122, and 8.232 are the weights, and 7.091 is the bias that was determined by the developed ANN model. Z_1 , Z_2 , and Z_3 are the dependent variables, which can be determined as a function of the five input parameters as follows

$$\begin{aligned} Z_1 &= 0.133 * D - 0.0002 * L + 4.262 * t + 0.035 * f_y \\ &+ 0.557 * f'_c - 95.502 \\ Z_2 &= 0.142 * D - 2.8 * 10^{-5} * L + 1.741 * t + 0.051 * f_y \\ &+ 0.399 * f'_c - 57.647 \\ Z_3 &= 0.106 * D - 0.002 * L + 1.219 * t + 0.011 * f_y \\ &+ 0.112 * f'_c - 12.372 \end{aligned} \quad (22)$$

6.2 Comparison with the given equations

The accuracy of the proposed equation (Eq. (21)) is compared against some empirical equations presented in the well-known design codes. Moreover, the ANN estimation accuracy is benchmarked against two intelligent models, including the Multiple Linear Regression (MLR), and the Decision Tree (DT). Again, the criteria presented in Section 4.1 are used for this comparison.

Table 5 Weight values and biases of the optimal ANN model

Neuron	Weights					Bias		
	Input			Output		Hidden layer	Output layer	
	D	L	t	f_y	f_c'	N_u		
1	12.825	-0.153	11.572	4.943	5.151	10.731	-24.464	7.091
2	13.656	0.019	4.727	7.229	3.691	5.122	-5.947	
3	10.179	-1.397	3.309	1.522	1.033	8.232	16.225	

Table 6 Comparison of ANN model with empirical equations

Criterion	Unit	ACI	EC4	AIJ	MLR	DT	ANN
MSE	$\times 10^5 \text{ KN}^2$	3.870	10.873	1.299	3.287	0.864	0.328
RMSE	$\times 10^3 \text{ kN}$	0.062	0.104	0.036	0.573	0.029	0.018
MAPE		0.260	0.441	0.243	1.022	0.192	0.190
MAE	$\times 10^3 \text{ kN}$	0.403	0.617	0.244	0.421	0.196	0.189
R		0.988	0.987	0.989	0.956	0.989	0.992
VAF	%	95.415	86.297	97.800	91.89	98.11	98.23

Table 6 compares the performance between the proposed equation in this study and three other empirical equations from the current design codes. It is shown that in every criterion, the proposed equation shows an outstanding accuracy compared to the others, and the EC4's equation shows the lowest accuracy. The correlation coefficient, R, obtained from ANN models equal to 0.992, which indicates a high performance and a good correlation between the measured and the predicted compressive strength. In contrast, the R-values are obtained from the available design codes and the other models, which have ranging from 0.956 to 0.989. The absolute percentage error, MAPE, obtained from the ANN model equal to 19% whereas these values of design codes equal to 26%, 44.1%, and 24.3%, respectively, and 42.1% and 19% for the MLR and the DT. The results from other criteria also show similar demonstrations.

Graphically, Fig. 10 shows a comparison of performance between the different equations in terms of the linear correlation coefficient. If data points cluster closely around a diagonal line (fit line), it represents the best correlation between the predicted and the experimental values. Fig. 10(a) shows that the given equation by the EC4 gives overestimated results, and the lowest underestimation performance is observed from the ACI equation in Fig. 10(b). On the other hand, the AIJ equation tends to both over-estimate and under-estimate the axial compressive capacity with the R values of 0.989, which is shown in Fig. 10(c). Fig. 10(d) indicates that the MLR model gives over-estimated results with an R-value of 0.956. Moreover, some below zero results are predicted by the MLR model. This trend is also true for the DT model in Fig. 10(e), but the proposed ANN equation produces a higher coefficient R of

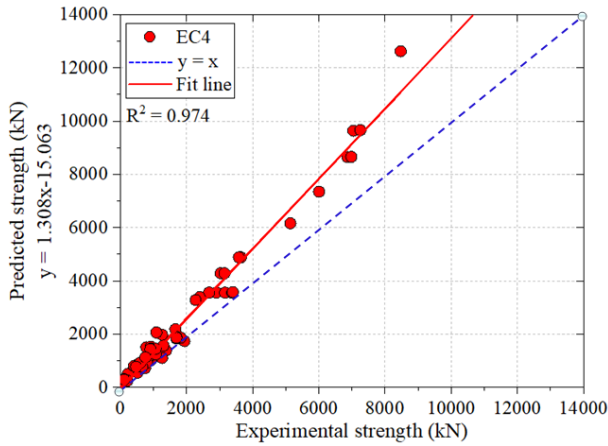
0.993 (Fig. 10(f)). The analysis shows that the predicted capacity of the proposed ANN equation is better than the other empirical equations and the other intelligent models. Generally, the proposed equation obtains superior results among the empirical equations with all four criteria.

6.3 The influence of the variables on experimental-to-predicted strength ratio

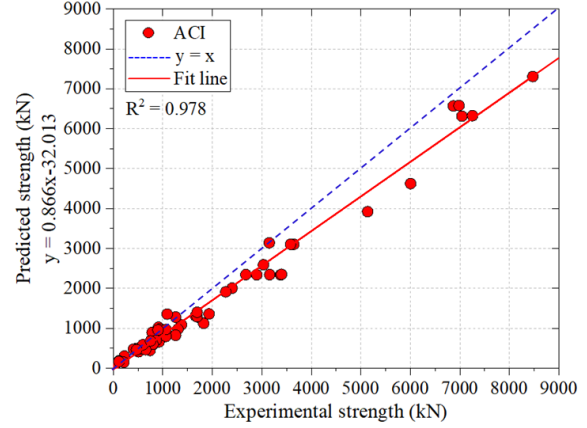
In this section, the ANN method and the design codes are considered to further investigate the effect of some of the variables on the predicted compressive strengths. Many important variables affected the compressive behavior of the CFST columns, which include the concrete strength, the steel strength, the length of the column, the diameter of the column, the length-to-diameter ratio, and the diameter-to-thickness ratio. In the Figs. (11)-(14), the normalized values ($N_{u, \text{ predicted}}/N_{u, \text{ experimental}}$) versus the prediction parameters are illustrated to indicate the effectiveness of the prediction parameters. The most accurate prediction performance is marked as a normalized value of 1.0

6.3.1 Effect of the concrete strength

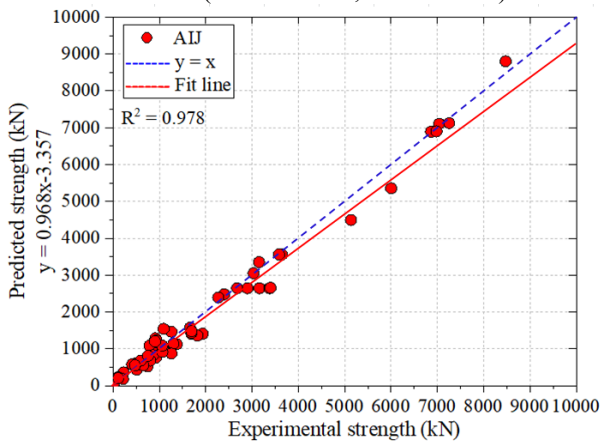
The variation of the experimental-to-predicted compressive strength ratio versus the concrete compressive strength for each method is shown in Figs. 11(a)-11(f). From these figures, it is clear that the EC4 method yielded scattered results for the investigated range. For the ACI and the AIJ method, this ratio illustrates less scatter. This analysis is also evaluated on the COV index. The COV is the coefficient of the variance. The COV of the ACI and the AIJ are 0.368, 0.397, and the EC4 is 0.397. As a result, the reliability indexes of the AIJ and the ACI are higher than



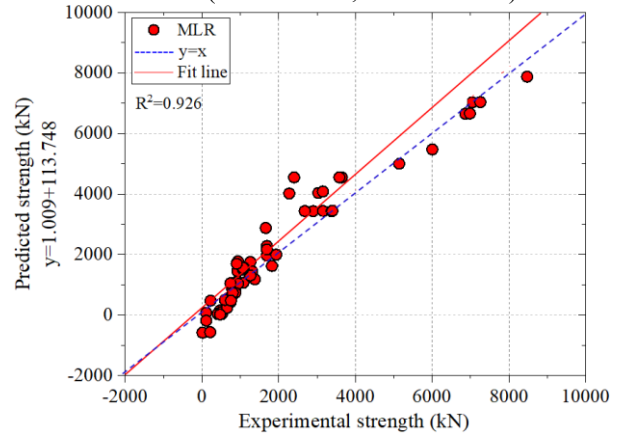
(a) EC4 performance
(Mean= 1.425, COV=0.397)



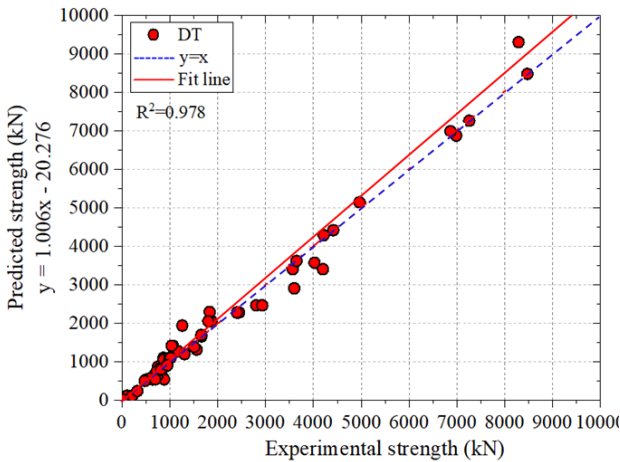
(b) ACI performance
(Mean=0.930, COV = 0.368)



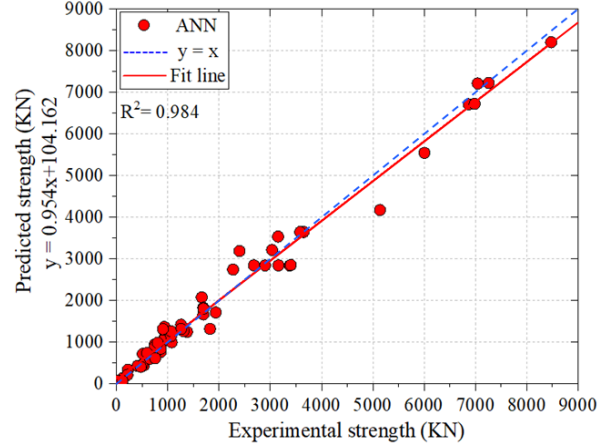
(c) AIJ performance
(Mean = 1.065, COV=0.397)



(d) MLR performance
(Mean = 20.937 , COV = 5.789)



(e) Decision Tree performance
(Mean = 0.989 , COV = 0.161)



(f) Proposed equation performance
(Mean = 1.049, COV = 0.161)

Fig. 10 Comparison of predicted versus experimental strengths between various equations

EC 4 index. Also, the MLR model gives a less accurate performance when predicted with some underestimated values, which is shown in Fig. 11(d). The results of the ultimate compressive strength ratios using the DT and the ANN model indicate consistent accuracy for the range of the concrete strength being investigated, which is shown in Figs. 11(e)-11(f).

6.3.2 Effect of the concrete strength

Figs. 12(a)-12(f) displays the effect of the yield strength of steel on the ultimate compressive strength ratio for the ANN models, as well as the ACI, the EC4, the AIJ, and other models as MLR and DT. The ultimate compressive strength ratios using the AIJ and the ACI show less scatter when the value of the ratio ranging between 0.5 and 3.

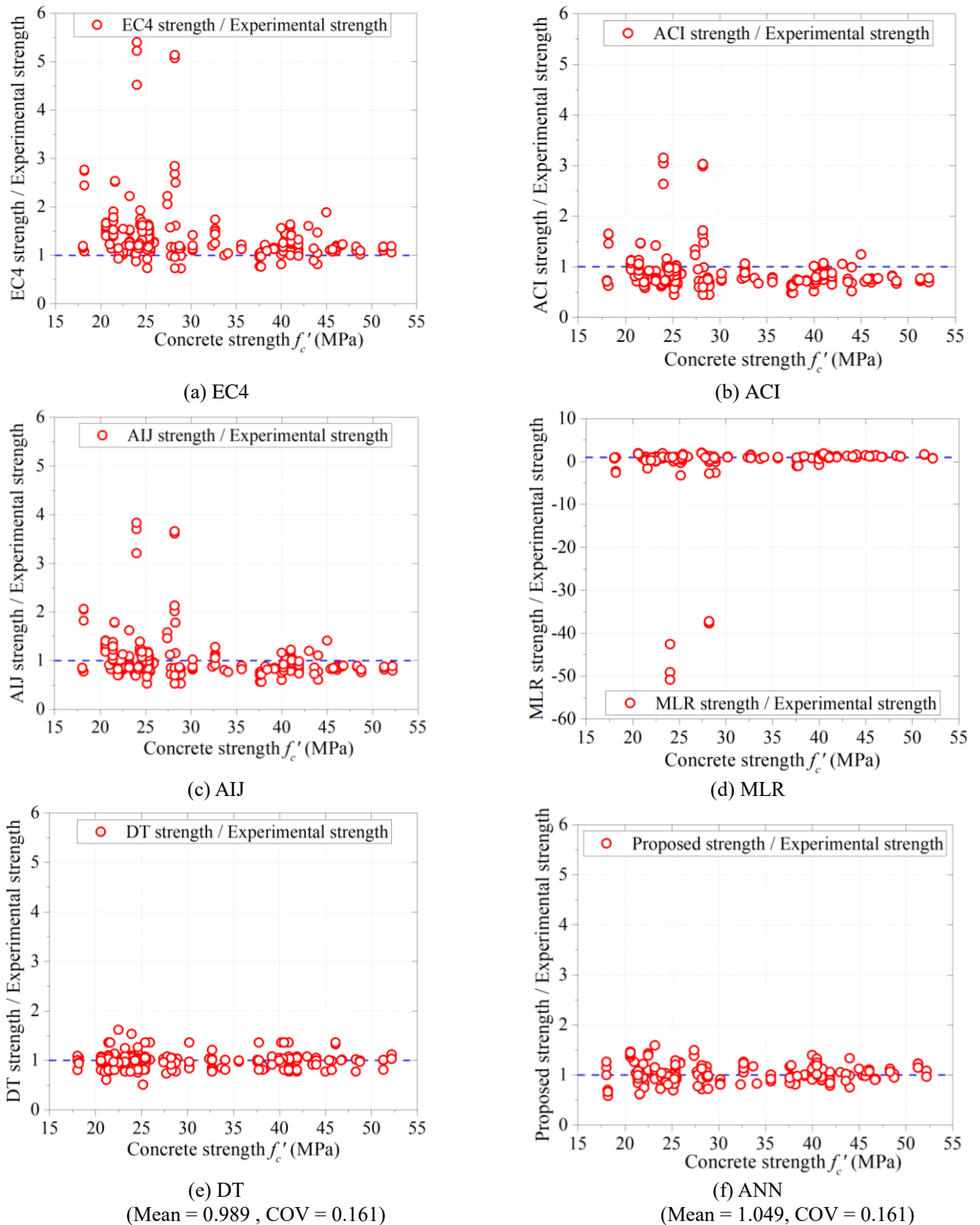


Fig. 11 Variation of experimental to predicted compressive strength ratio with concrete strength using different methods

Whereas the EC4 gives a result and shows more scatter comparing with the ACI and the AIJ. Also, it tends to be very conservative with the experimental observations that range from 0.5 to 5.5. For intelligent models, this ratio is greater than -30 in the MLR model, whereas these ratios for

DT and ANN models are just around 1.0. Furthermore, the results also showed that all design codes show a lot of dispersion in the case with high strength steel. In contrast, the ANN results are not affected more by the variations in steel strength.

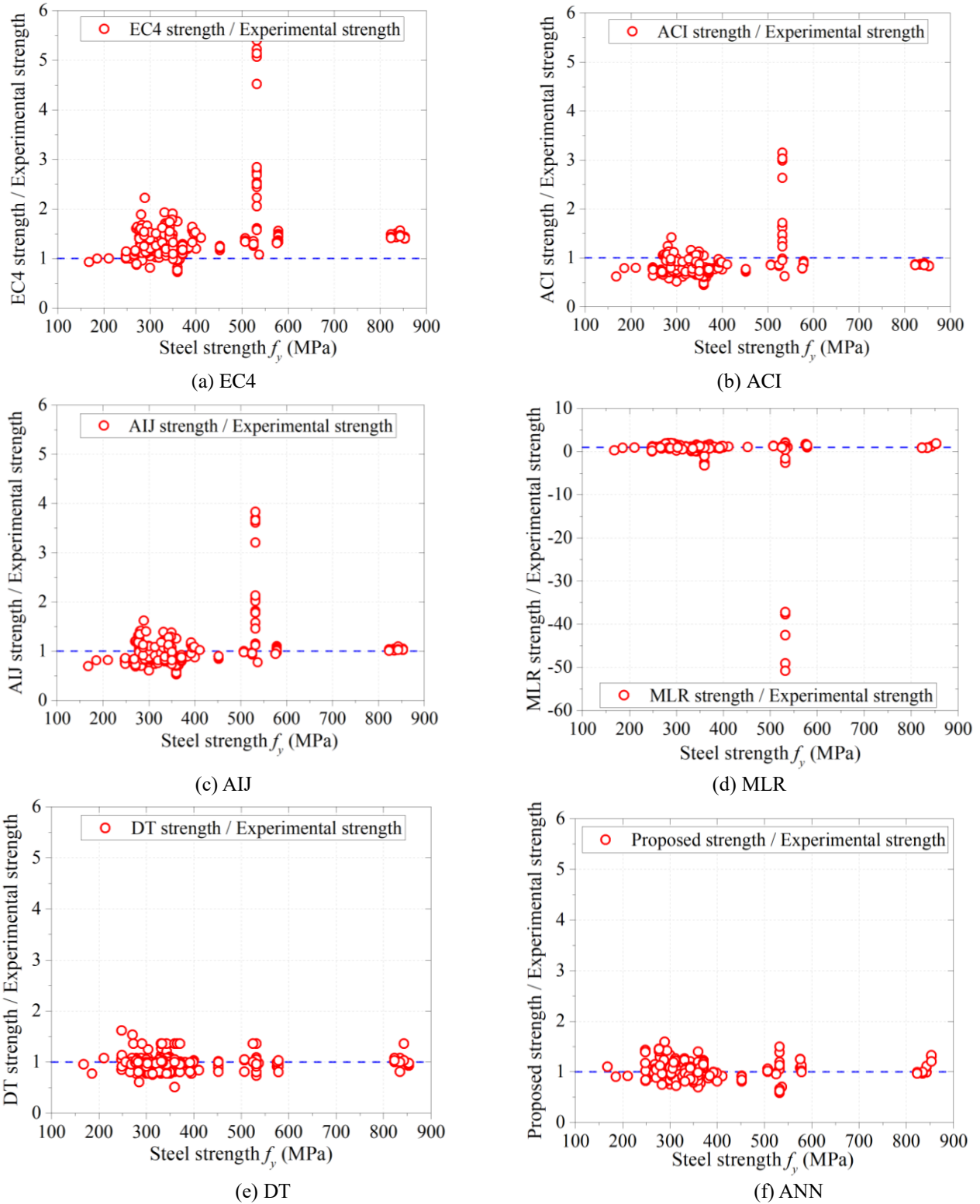


Fig. 12 Variation of experimental to predicted compressive strength ratio with steel strength using different methods

6.3.3 Effect of the diameter to thickness ratio (D/t)

The effect of the diameter-to-thickness ratio on the predicted results is presented in Figs. 13(a)-13(f). As expected, the ANN predicted results are in reasonably good agreement with all the ratios of D/t considered in this investigation. The ANN gives the closest predictions with

an average value (μ) of 1.05, while the ACI, AIJ, EC4, and MLR show lots of scattering and conservatism with a mean value (μ) of 0.93, 1.07, 1.43, and 20.94, respectively. For all the design codes, the bearing capacity may not be predicted correctly if using the diameter to thickness ratios is smaller than 30. Moreover, in design codes, the limitations of the

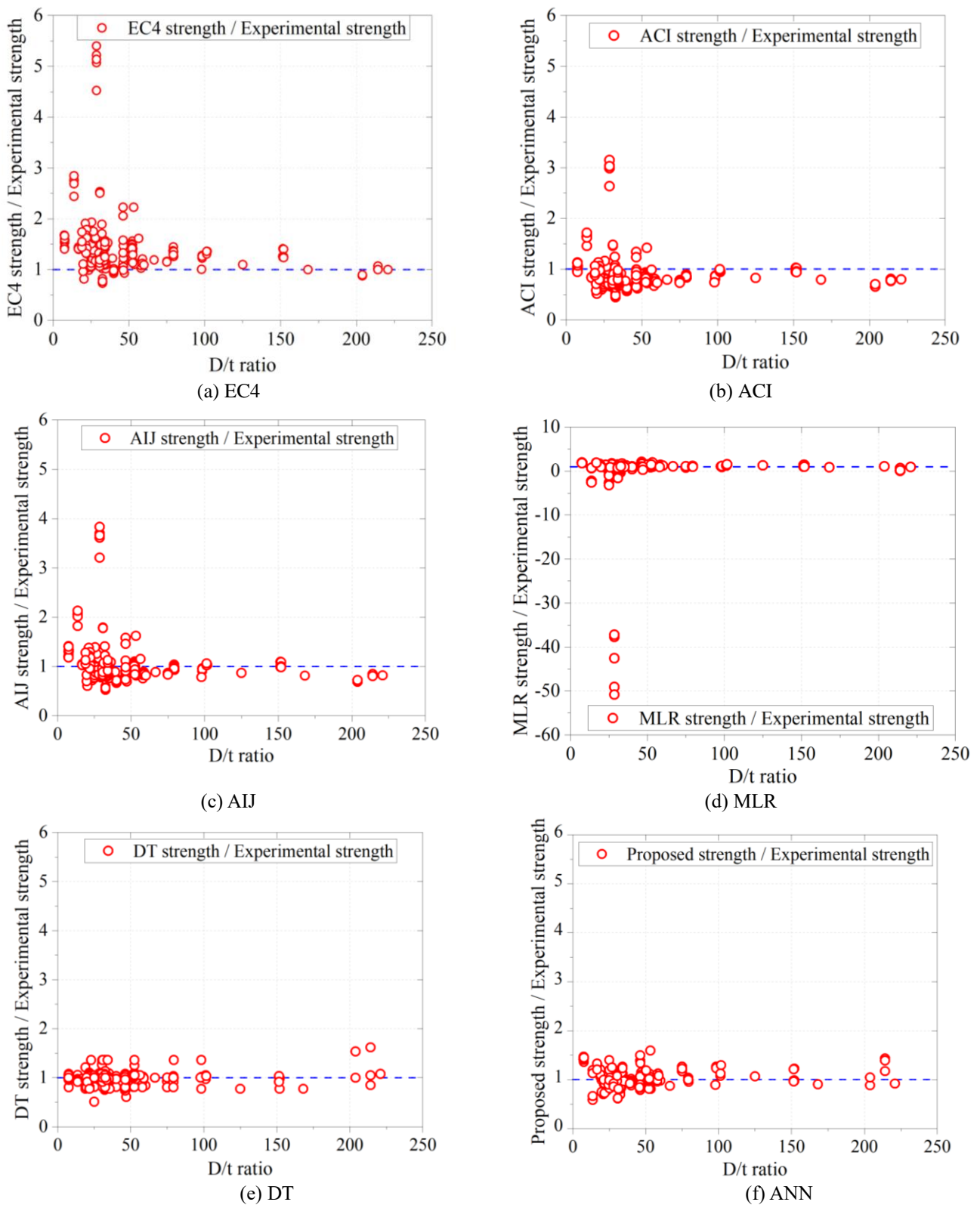


Fig. 13 Variation of experimental to predicted compressive strength ratio with diameter-to-thickness ratio using different methods

diameter to thickness ratio also exist, which is not convenient for the design. Namely, the width to thickness

ratio cannot exceed $\sqrt{8Es/f_y}$, $90 \frac{235}{f_y}$ in ACI and EC4

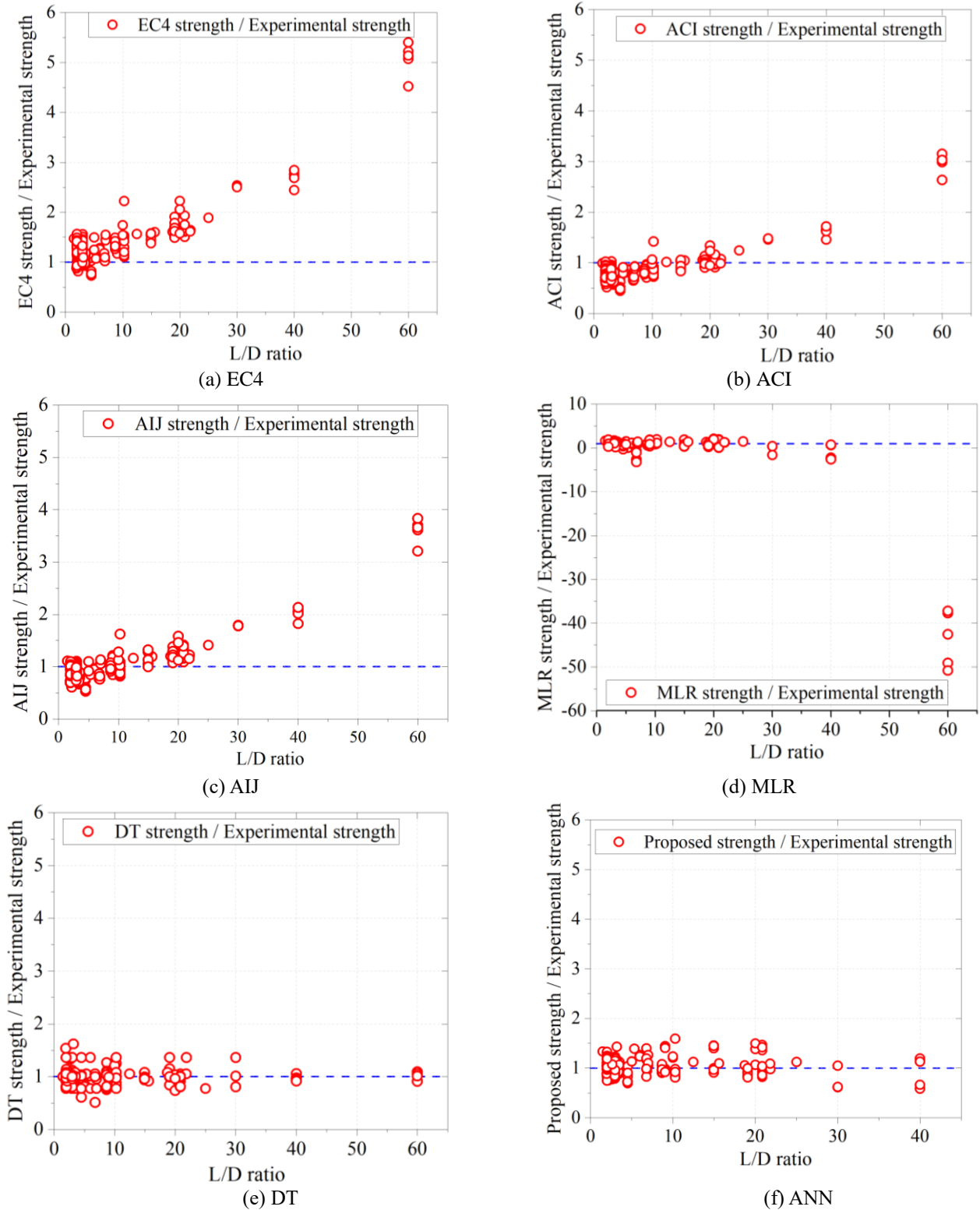


Fig. 14 Variation of experimental to predicted compressive strength ratio with length-to-diameter ratio using different methods

respectively, which E_s is the elasticity modulus of steel, and f_y is the steel strength. In contrast, the ANN model provided a wide application range to design the CFST columns.

6.3.4 Effect of the length to diameter ratio (L/D)

The variations of the ultimate compressive strength ratios with the L/D values are shown in Figs.14 (a)-14(f). For the slender columns ($L/D > 4$) in three design codes, it

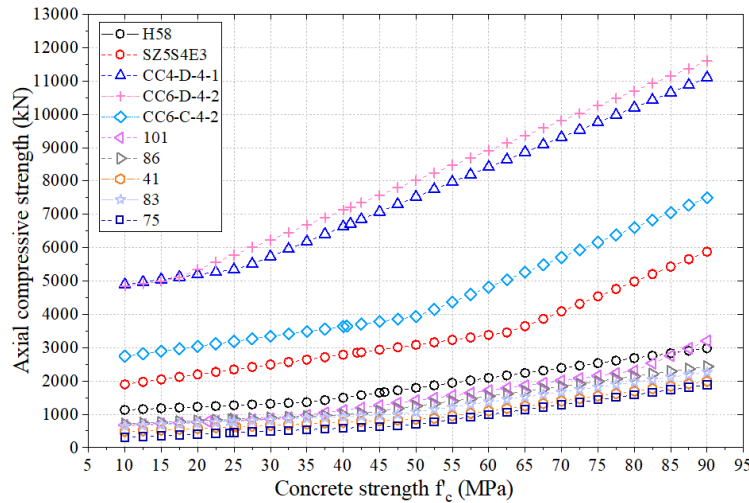


Fig. 15 Effect of concrete strength on axial compressive capacity

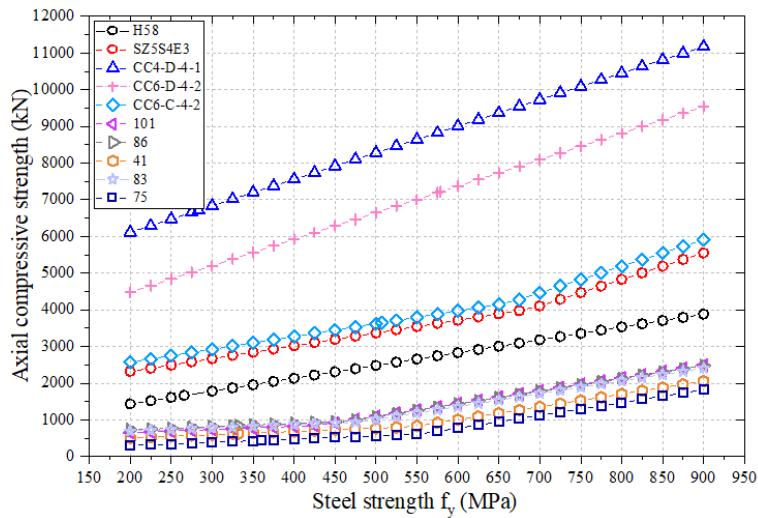


Fig. 16 Effect of steel strength on axial compressive capacity

is provided poor results with strong scattering predictions that predicted-to-experimental strength ratios ranging from 1.0 to 5.5. Moreover, some points are too under-estimated in the MLR model with the ratio range overcome -50.0. This means that the local buckling effect in slender columns should be carefully considered for design codes. In contrast, the results obtained from the DT and the ANN model show accuracy and consistency for all values of L/D being investigated.

7. Parametric study for proposed ANN model

To further examine the generalization ability or the robustness of the ANN model, the parametric study is carried out that demonstrates the response of the predicted model's ultimate compressive strength to a set of hypothetical input parameters. The effect of one input variable is examined by allowing it to adjust while all other

input variables are set to fixed values. The inputs are then accommodated in the ANN model, and the predicted ultimate compressive strength is calculated. This process is repeated for the next input variable and so on until the model response has examined all the parameters. A summary of the material strengths and the geometric dimensions of the representative tests for evaluating is presented in Table 7. The results of the sensitivity analysis are shown in the sub-section.

7.1 The concrete strength

The effect of the first parametric study on the ultimate compressive strength of the circular CFST columns is presented shown in Fig. 15. This parametric study is carried out by changing the values of the concrete strength while keeping the other input parameters constant. Ten different specimens are used in the parametric study, including 5 slender columns and 5 short columns. Fig. 15 exhibits the

Table 7 Summary of representative experimental specimens

Member type	Numbering of specimens	D (mm)	L (mm)	L/D	t (mm)	D/t	f_y (MPa)	f'_c (MPa)
Short column ($L/D \leq 4$)	H58	174	360	2.07	3	58	265.9	45.68
	SZ5S4E3	219	650	2.97	4.73	4.63	350	41.
	CC4-D-4-1	449.8	1348.7	3	2.97	151.45	283.4	41
	CC6-D-4-2	360.2	1079.5	3	4.55	79.165	578.5	41
	CC6-C-4-2	238	476	2	4.54	52.423	507	40.5
Slender column ($L/D > 4$)	101	121	2310	19.1	5.69	21.265	349	21.4
	86	121	1050	8.68	3.99	30.326	332	24.6
	41	95	860	9.05	3.66	25.956	332	25.3
	83	121	1050	8.68	3.66	33.06	300	24.4
	75	95	1980	20.8	3.58	26.536	360	24.4

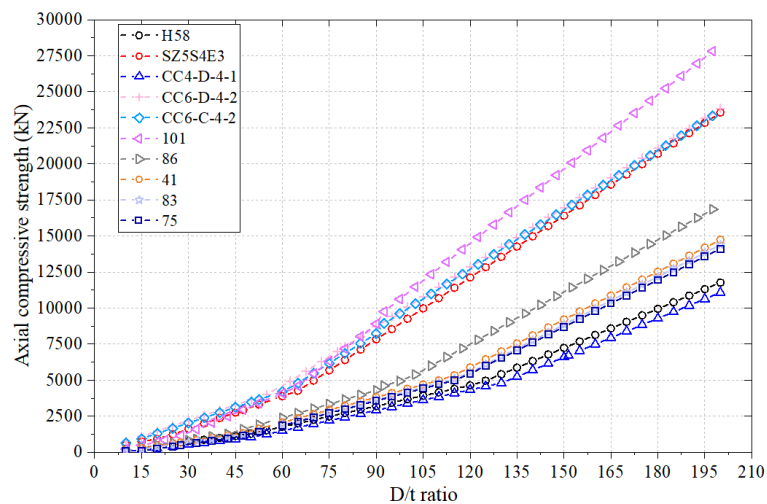


Fig. 17 Effect of diameter-to-thickness ratio on axial compressive capacity

curves with different concrete strengths. It is shown that increasing concrete strength leads to increasing the compressive strength of the CFST columns. Specifically, the compressive strength of column slowly increases when concrete strength is raised by 10 to 25 MPa for the short columns; if the columns use concrete strengths ranging from 25 to 90 MPa, the compressive strength of CFST column can be rapidly increased by 185%. Besides, it is observed that the concrete strength increases insignificantly when the concrete strength is increased from 10 to 50 MPa for the slender columns. The growth becomes to increase rapidly after that at a rate of 103% during 50-90 MPa of the concrete strength. This indicated that the increase in concrete strength leads to the constraint effect increasing.

7.2 The steel strength

The second parametric study is carried out to show the variation of the ultimate compressive strength on circular CFST columns as steel strength. The results of this second

parametric study are presented in Fig. 16. According to all of the curves, it indicated that the axial compressive strength is proportional to the steel strength.

7.3 The diameter-to-thickness ratio (D/t)

The diameter-to-thickness ratio also special affects the bearing capacity. To ensure the steel tubes and the concrete work as integral, the evaluation of the diameter to thickness ratio was considered. The results of the variation in the bearing capacity versus the diameter to thickness ratio are illustrated in Fig. 17. Based on obtained results, it indicated that the compressive strength raises the stability with the ratio ranging from 10 to 70. After that, the bearing strength increases significantly as the diameter-to-thickness ratio increase from 70 to 200 as a result of the strong constraint effect. The main reason comes from the hoop or circumferential stress. A higher hoop or circumferential stress results in a significantly increased load-carrying capacity of the CFST columns.

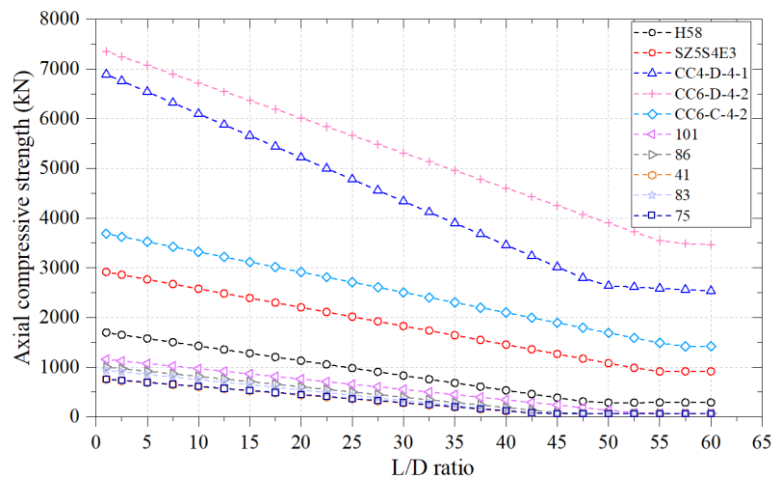


Fig. 18 Effect of length-to-diameter ratio on axial compressive capacity

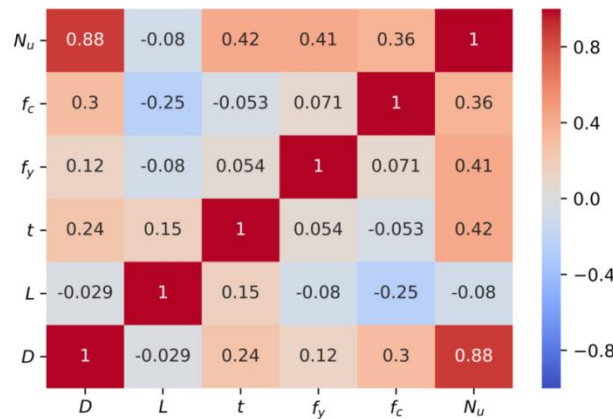


Fig. 19 Spearman correlation matrix between each input and output parameters

7.4 The length to diameter ratio (L/D)

As shown in Fig. 18, the compressive strength of the column decreases when the length-to-diameter ratio increases. The ultimate strength decreases when the length-to-diameter ratio is lower than 50. In contrast, the strength does not change when the ratio for slender columns reaches 50. The short columns tend to the same result when the length-to-diameter ratio was larger than 50 (CC4-D-4-1 and H58) and 55 (SZ5S4E3, CC6-D-4-2, CC6-C-4-2). It can be seen the effect of the confinement effect is reduced with the increasing length to thickness ratio, because of the lateral deflection before the failure increases the bending moment and reduces the mean compressive strain in the concrete.

8. Spearman’s correlation coefficient

The relationship of pair parameters was evaluated using the Spearman’s correlation coefficient. The Spearman correlation coefficient is a monotonic nonparametric

technique that is used to summarize the strength and the direction, which can be positive or negative, of the correlation between two parameters. The level of interaction is called significant (or very strong) if the coefficient scale is between 0.8 and 1. High (or strong) between 0.5 and 0.8 and moderate (or fair) between 0.2 and 0.5, and very small (or poor) below 0.2. If the coefficient is equal to 0, the two variables are independent of one another. When it is equal to 1 they are perfectly correlated in a positive way, whereas when it is equal to -1 the variables are perfectly correlated negatively (anti-correlation). The Spearman correlation matrix is given in Fig. 19. According to the results of Spearman correlation matrix, It is clear that the axial compressive strength is highly influenced by D , followed by f_c , t , f_y , and L . This conclusion can help researchers and designers make appropriate decisions on reality designing.

9. Conclusions

A novel prediction model used to obtain an explicit

predicted formulation of ultimate compressive capacity (N_u) of the concrete filled steel tube (CFST) column using ANN is presented in this study. The available experimental data were collected from the technical literature for developing the model. The following conclusions have been drawn from this study.

- (1) The Artificial Neural Network was efficiently employed to predict the axial compressive capacity of a CFST column, and it obtained superior results with a high level of confidence. The predicted results demonstrated the robustness and the effectiveness of the proposed ANN model, which can be applied for similar problems in structural and civil engineering.
- (2) For the convenience of the practical design, an empirical equation was proposed from the model. It showed that the compressive strength obtained from the proposed equation is more accurate than the compressive strength obtained from the well-known design codes. This can be explained that the proposed ANN model took into account all five-input variables' effect on the compressive strength of CFST column. It is noteworthy that the range of applicability of the derived equation is restricted by the used data. Consequently, if the input values are outside these ranges, the proposed ANN model should be used with caution.
- (3) To investigate the effects of the input variables, a parametric study was performed. The parametric study showed that learning of the ANN was significantly dependent on the given set of training data, and the results confirmed that the reliability can be improved based on the ANN. Besides, the study also indicated that the diameter of column (D) is the most important parameter regarding the axial compressive strength.

Acknowledgments

This research described in this paper was financially supported by the National Research Foundation of Korea (NRF) grant funded by the Korean government (MSIT) (No.2018R1A2A2A05018524 and No. 2019R1A4A1021702).

References

- Abed, F., Alhamaydeh, M. and Abdalla, S. (2013), "Experimental and numerical investigations of the compressive behavior of concrete filled steel tubes (CFSTs)", *J. Constr. Steel Res.*, **80**, 429-439. <https://doi.org/10.1016/j.jcsr.2012.10.005>.
- AIJ. Recommendations for design and construction of concrete filled steel tubular structures, (1997). Architectural Institute of Japan, Tokyo.
- Altun, F., Kişi, Ö. and Aydın, K. (2008), "Predicting the compressive strength of steel fiber added lightweight concrete using neural network", *Comput. Mater. Sci.*, **42**(2), 259-265.
- American concrete institute, (1962), *ACI 318. Building code requirements for structural concrete and commentary* (Vol. 552). USA.
- Aslani, F., Lloyd, R., Uy, B., Kang, W.H. and Hicks, S., (2016), "Statistical calibration of safety factors for flexural stiffness of composite columns", *Steel Compos. Struct.*, **20**(1), 127-145. <https://doi.org/10.12989/scs.2016.20.1.127>.
- Aslani, F., Uy, B., Tao, Z. and Mashiri, F., (2015), "Predicting the axial load capacity of high-strength concrete filled steel tubular columns", *Steel Compos. Struct.*, **19**(4), 967-993. <https://doi.org/10.12989/scs.2015.19.4.967>.
- Aslani, F., Uy, B., Wang, Z. and Patel, V., (2016), "Confinement models for high strength short square and rectangular concrete-filled steel tubular columns", *Steel Compos. Struct.*, **22**(5), 937-974. <https://doi.org/10.12989/scs.2016.22.5.937>.
- Beck, A.T., de Oliveira, W.L.A., De Nardim, S. and ElDebs, A.L. H. C., (2009), "Reliability-based evaluation of design code provisions for circular concrete-filled steel columns", *Eng. Struct.*, **31**(10), 2299-2308. <https://doi.org/10.1016/j.engstruct.2009.05.004>.
- Cheng, M.Y. and Cao, M.T. (2014), "Evolutionary multivariate adaptive regression splines for estimating shear strength in reinforced-concrete deep beams", *Eng. Appl. Artif. Intell.*, **28**, 86-96.
- Dantas, A.T.A., Batista Leite, M. and De Jesus Nagahama, K. (2013), "Prediction of compressive strength of concrete containing construction and demolition waste using artificial neural networks", *Constr. Build. Mater.*, **38**, 717-722. <https://doi.org/10.1016/j.conbuildmat.2012.09.026>.
- Das, S. and Choudhury, S. (2019), "Influence of effective stiffness on the performance of RC frame buildings designed using displacement-based method and evaluation of column effective stiffness using ANN", *Eng. Struct.*, **197**, 109354. <https://doi.org/10.1016/j.engstruct.2019.109354>.
- Duan, Z.H., Kou, S.C. and Poon, C.S. (2013), "Prediction of compressive strength of recycled aggregate concrete using artificial neural networks", *Constr. Build. Mater.*, **40**, 1200-1206. <https://doi.org/10.1016/j.conbuildmat.2012.04.063>.
- Ekmekyapar, T. and Ghanim Hasan, H. (2019), "The influence of the inner steel tube on the compression behaviour of the concrete filled double skin steel tube (CFDST) columns", *Mar. Struct.*, **66**, 197-212. <https://doi.org/10.1016/j.marstruc.2019.04.006>.
- Eurocode 4: Design of composite steel and concrete structures. Part 1.1, General rules and rules for buildings. EN 1994-1-1:2004, (2004). Brussels.
- Furlong, R.W. (1967), "Strength of steel-encased concrete beam columns", *J. Struct. Div.*
- Giakoumelis, G. and Lam, D. (2004), "Axial capacity of circular concrete-filled tube columns", *J. Constr. Steel Res.*, **60**(7), 1049-1068. <https://doi.org/10.1016/j.jcsr.2003.10.001>.
- Goode, C.D. (2008), "Composite Columns - 1819 Tests on Concrete-Filled Steel Tube Columns Compared with Eurocode 4", *Inst. Struct. Eng.*, **86**, 33-38.
- Gupta, P.K., Sarda, S.M. and Kumar, M.S. (2007), "Experimental and computational study of concrete filled steel tubular columns under axial loads", *J. Constr. Steel Res.*, **63**(2), 182-193.
- Hasan, H.G., Ekmekyapar, T. and Shehab, B.A. (2019), "Mechanical performances of stiffened and reinforced concrete-filled steel tubes under axial compression", *Mar. Struct.*, **65**, 417-432. <https://doi.org/10.1016/j.marstruc.2018.12.008>.
- Hayashi, F. (1990), *Study on mechanical behavior of circular confined concrete column under axial compression*. Kyushu University.
- Hwang, H.J., Baek, J.W., Kim, J.Y. and Kim, C.S. (2019), "Prediction of bond performance of tension lap splices using artificial neural networks", *Eng. Struct.*, **198**, 109535. <https://doi.org/10.1016/j.engstruct.2019.109535>.
- Ioffe, S. (2017), "Batch renormalization: Towards reducing minibatch dependence in batch-normalized models", *Proceedings of the 31st Conference on Neural Information Processing Systems (NIPS 2017)*, Long Beach, CA, USA.
- Kang, J.Y., Choi, B.I. and Lee, H.J. (2006), "Application of artificial neural network for predicting plain strain fracture

- toughness using tensile test results”, *Fatigue Fract. Eng. Mater. Struct.*, **29**(4), 321-329. <https://doi.org/10.1111/j.1460-2695.2006.00994.x>.
- Ketkar, N., (2017), *Deep Learning with Python - A Hands-on Introduction*. <https://doi.org/10.1007/978-1-4842-2766-4>.
- Larocca, C.B., Farias, C.T.T., Simas Filho, E.F. and Silva, I.C. (2018), “Wall thinning characterization of composite reinforced steel tube using frequency-domain PEC technique and neural networks”, *J. Nondestruct. Eval.*, **37**(3), 1-8. <https://doi.org/10.1007/s10921-018-0477-1>.
- Lee, S. and Lee, C. (2014), “Prediction of shear strength of FRP-reinforced concrete flexural members without stirrups using artificial neural networks”, *Eng. Struct.*, **61**, 99-112. <https://doi.org/10.1016/j.engstruct.2014.01.001>.
- Li, Y., Han, L., Xu, W. and Tao, Z. (2016), “Circular concrete-encased concrete-filled steel tube (CFST) stub columns subjected to axial compression”, *Mag. Concr. Res.*, **68**(19), 995-1010. <https://doi.org/10.1680/jmacr.15.00359>.
- Lin, C.Y. (1988), “Axial capacity of concrete infilled cold-formed steel columns”, *Proceedings of the 9th International Specialty Conference on Cold-Formed Steel Structures*, 443-457. St. Louis, Missouri, U.S.A.
- Luat, N.V., Lee, K. and Thai, D.K. (2020), “Application of artificial neural networks in settlement prediction of shallow foundations on sandy soils”, *Geomech. Eng.*, **20**(5), 385-397. <https://doi.org/10.12989/gae.2020.20.5.385>.
- Luat, N.V., Lee, J., Lee, D.H. and Lee, K. (2020), “GS - MARS method for predicting the ultimate load - carrying capacity of rectangular CFST columns under eccentric loading”, *Comput. Concret.*, **25**(1), 1-14. <https://doi.org/10.12989/cac.2020.25.1.001>.
- Luksha, L.K. and Nesterovich, A.P. (1991), “Strength testing of large-diameter concrete filled steel tubular members”, *Proceedings of the Third International Conference on Steel-Concrete Composite Structures, ASCCS, Fukuoka*, 67-70.
- Moon, J., Kim, J.J., Lee, T.H. and Lee, H.E. (2014), “Prediction of axial load capacity of stub circular concrete-filled steel tube using fuzzy logic”, *J. Constr. Steel Res.*, **101**, 184-191.
- Nikoo, M., Zarfam, P. and Sayahpour, H. (2013), “Determination of compressive strength of concrete using Self Organization Feature Map (SOFM)”, *Eng. Comput.*, **31**(1), 113-121. <https://doi.org/10.1007/s00366-013-0334-x>.
- Oliveira, W.L.A. (2008), *Theoretical-experimental analysis of circular concrete filled steel columns*, Doctoral thesis. São Carlos School.
- O’Shea, M.D. and Bridge, R.Q. (2000), “Design of Circular Thin-Walled Concrete Filled Steel Tubes”, *J. Struct. Eng.*, **126**(11), 1295-1303.
- Knowles, R.B. and Park, R. (1970), “Axial load design for concrete filled steel tubes”, *J. Struct. Div.*, **96**(10), 2125-2153.
- Sakino, K., Nakahara, H., Morino, S. and Nishiyama, I. (2004), “Behavior of centrally loaded concrete-filled steel-tube short columns”, *J. Struct. Eng.*, **130**(2), 180-188.
- Salani, H.J. and Sims, J.R. (1964), “Behavior of Mortar Filled Steel Tubes in Compression”, *J. Proceedings*, 1271-1284.
- Schneider, S.P. (1998), “Axially loaded concrete-filled steel tubes”, *J. Struct. Eng.*, **124**(10), 1125-1138. [https://doi.org/10.1061/\(ASCE\)0733-9445\(1999\)125:10\(1202\)](https://doi.org/10.1061/(ASCE)0733-9445(1999)125:10(1202)).
- Shanmugam, N.E. and Lakshmi, B. (2001), “State of the art report on steel-concrete composite columns”, *J. Constr. Steel Res.*, **57**(10), 1041-1080. [https://doi.org/10.1016/S0143-974X\(01\)00021-9](https://doi.org/10.1016/S0143-974X(01)00021-9).
- Tang, C.W. (2017), “Fire resistance of high strength fiber reinforced concrete filled box columns”, *Steel Compos. Struct.*, **23**(5), 611-621. <https://doi.org/10.12989/scs.2017.23.5.611>.
- Tao, Z., Han, L.H. and Wang, L.L. (2007), “Compressive and flexural behaviour of CFRP-repaired concrete-filled steel tubes after exposure to fire”, *J. Constr. Steel Res.*, **63**(8), 1116-1126. <https://doi.org/10.1016/j.jcsr.2006.09.007>.
- Tomii, M. (1977), “Experimental studies on concrete filled steel tubular stud columns under concentric loading”, *Proceedings of the International Colloquium on Stability of Structures Under Static and Dynamic Loads*, 718-741. Washington, DC.
- Uy, B. (2001), “Strength of short concrete filled high strength steel box columns”, *J. Constr. Steel Res.*, **57**(2), 113-134. [https://doi.org/10.1016/S0143-974X\(00\)00014-6](https://doi.org/10.1016/S0143-974X(00)00014-6).
- Varma, A.H., Ricles, J.M., Sause, R. and Lu, L.W. (2002), “Seismic behavior and modeling of high-strength composite concrete-filled steel tube (CFT) beam-columns”, *J. Constr. Steel Res.*, **58**(5-8), 725-758. [https://doi.org/10.1016/S0143-974X\(01\)00099-2](https://doi.org/10.1016/S0143-974X(01)00099-2).
- Wang, L., Cao, X.X., Ding, F.X., Luo, L., Sun, Y., Liu, X.M., and Su, H.L. (2018), “Composite action of concrete-filled double circular steel tubular stub columns”, *Steel Compos. Struct.*, **29**(1), 77-90. <https://doi.org/10.12989/scs.2018.29.1.077>.
- Xiao, Y. (1989), *Experimental Study and Analytical Modeling of Triaxial Compressive Behavior of Confined Concrete*, Ph.D. Thesis, Kyushu University, Fukuoka, Japan.
- Yamamoto, T., Kawaguchi, J. and Morino, S., (2000), “Scale Effects on Compressive Behavior of Concrete-Filled Steel Tube Short Columns”, *Compos. Constr. Steel Concr. IV*, **25**, 27-44. [https://doi.org/10.1061/40616\(281\)76](https://doi.org/10.1061/40616(281)76).
- Yaseen, Z.M., Tran, M.T., Kim, S., Bakhshpoori, T. and Deo, R.C. (2018), “Shear strength prediction of steel fiber reinforced concrete beam using hybrid intelligence models: A new approach”, *Eng. Struct.*, **177**, 244-255.
- Yoshioka, K., Inai, E., Hukamoto, N., Kai, M. and Murata, Y. (1995), “Compressive Tests on CFT Short Columns Part 1: Circular CFT Columns”, *Proceedings of the 2nd Jt. Tech. Coord. Comm. Compos. Hybrid Struct. Phase 5 Compos. Hybrid Struct.*
- Yu, Q., Tao, Z. and Wu, Y.X. (2008), “Experimental behaviour of high performance concrete-filled steel tubular columns”, *Thin-Wall. Struct.*, **46**(4), 362-370.
- Zeghiche, J. and Chaoui, K. (2005), “An experimental behaviour of concrete-filled steel tubular columns”, *J. Constr. Steel Res.*, **61**(1), 53-66. <https://doi.org/10.1016/j.jcsr.2004.06.006>.

CC

Nomenclature

Notations

<i>CFST</i>	concrete filled steel tube
<i>ANN</i>	artificial neural network
<i>MLR</i>	multiple linear regression
<i>DT</i>	decision tree
<i>EC4</i>	Eurocode 4
<i>ACI</i>	American Concrete Institute
<i>AIJ</i>	Architectural Institute of Japan
<i>MAPE</i>	absolute percentage error
<i>MAE</i>	mean absolute error
<i>MSE</i>	mean squared error
<i>RMSE</i>	root mean squared error
<i>VAF</i>	variance accounted for
A_c	cross section area of concrete (mm ²)
A_s	cross section area of steel (mm ²)
f_c'	compressive strength of the concrete (MPa)
f_y	yield strength of steel (MPa)
D	diameter of the column (mm)
L	length of the column (mm)
t	thickness of steel tube (mm)
N_u	axial compressive capacity (kN)
η_c	coefficient of concrete confinement
η_a	coefficient of steel tube confinement
λ	relative slenderness
$N_{pl,R}$	characteristic value of the plastic resistance to compressive
N_{cr}	elastic critical normal force for relevant buckling mode
l	buckling length of the column
$(EI)_{eff}$	the effective flexural stiffness
K_e	correction factor $K_e=0.6$
E_{c2}	modulus of elasticity of concrete
η	confinement factor
l_k	effective length of the tube filled with concrete

Appendix

Table A Data of experimental axial compressive capacity

No of specimens	D (mm)	L (mm)	t (mm)	f_y (MPa)	f_c' (MPa)	N_u (kN)	References
8	25.40	216.00	0.89	168.21	18.04	14.40	Zeghiche (2005)
	115.02	300.50	5.02	365.00	46.10	1413.00	
3	140.00	635.00	3.00	285.00	18.18	881.00	Schneider (1998)
	141.40	635.00	6.68	537.00	23.81	2715.00	
3	152.40	914.40	1.55	331.00	21.00	682.40	Hayashi (1990)
	152.40	914.40	1.55	331.00	25.90	733.10	
3	150.00	480.00	0.70	248.20	22.50	513.50	Tomii <i>et al.</i> (1977)
	150.00	800.00	0.70	248.20	33.70	743.80	
12	238.00	713.70	2.97	283.40	25.40	3034.10	Salani and Sims (1964)
	450.10	1348.70	6.48	834.30	41.00	9832.30	
5	165.00	580.50	0.86	185.70	41.00	1350.00	Beck <i>et al.</i> (2009)
	190.00	664.50	2.82	363.30	48.30	1695.00	
3	114.00	250.00	3.60	300.00	44.00	1042.00	Xiao (1989)
	167.00	250.00	5.60	300.00	44.00	1710.00	
18	50.00	340.00	2.00	360.00	25.15	210.00	Knowles (1970)
	100.00	340.00	2.50	360.00	40.00	822.00	
27	108.00	216.00	2.96	279.00	25.40	941.00	Li <i>et al.</i> (2016)
	450.00	2000.00	6.47	853.00	41.10	9835.00	
5	159.90	2000.00	4.96	270.00	40.00	1091.00	Oliveira (2008)
	160.30	4000.00	5.00	281.00	45.00	1261.00	
11	165.00	341.00	1.00	248.50	22.06	1197.19	Yu <i>et al.</i> (2007)
	204.00	400.00	9.00	363.40	45.68	3000.00	
9	150.00	300.00	2.00	168.21	18.04	747.14	Giakoumelis and Lam (2004)
	150.00	300.00	4.29	311.17	28.73	1306.12	
4	300.00	900.00	4.50	348.10	32.36	4551.32	O'Shea (2000)
	300.00	900.00	11.88	400.10	35.60	7953.08	
46	95.00	860.00	3.40	277.00	20.60	413.00	Furlong (1967)
	216.00	2310.00	12.80	411.00	30.20	2932.00	
17	25.40	1524.00	0.89	532.00	18.20	14.40	Lin (1988)
	76.20	1524.00	2.77	532.00	28.30	320.30	
2	102.00	702.00	2.94	320.00	48.74	824.00	Luksha (1991)
	102.00	702.00	2.94	320.00	48.74	886.00	
26	101.30	305.00	3.03	335.00	23.20	632.00	Gupta <i>et al.</i> (2007)
	318.50	955.00	10.37	452.00	52.20	9297.00	
8	114.30	571.50	3.35	287.33	22.50	599.30	Yamamoto and Kawaguchi (2000)
	114.30	1143.00	6.00	342.95	32.68	1057.10	
9	165.00	510.00	2.75	350.00	34.10	1560.00	Sakino <i>et al.</i> (2004)
	219.00	650.00	4.78	350.00	41.90	3600.00	